

# Membrane Fusion

Robert Blumenthal,<sup>\*,†</sup> Michael J. Clague,<sup>‡</sup> Stewart R. Durell,<sup>†</sup> and Richard M. Epand<sup>§</sup>

Center for Cancer Research, National Cancer Institute, National Institutes of Health, Bethesda-Frederick, Maryland, Physiological Laboratory, University of Liverpool, Crown Street, Liverpool L69 3BX, UK, and Department of Biochemistry, McMaster University, Hamilton, Ontario, Canada L8N 3Z5

Received April 10, 2002

## Contents

I. Introduction	53
II. Membrane Fusion Assays	54
A. Liposomes as Models	55
B. Biological Membranes	56
1. Virus–Cell Fusion	56
2. Cell–Cell Fusion Mediated by Viral Proteins	56
3. Intracellular Fusion	56
III. Membrane Rearrangements Required for Fusion	57
A. Adhesion, Deformation, and Fusion of Bilayers	57
B. Membrane Curvature and Destabilization	57
IV. Viral Membrane Fusion	59
A. Structure of Native and Low pH Influenza Hemagglutinin (HA)	59
B. Conformational Changes in Influenza HA	61
C. The Influenza HA-Mediated Fusion Cascade	61
V. Cellular Fusion	63
A. SNAREs	63
B. Other Factors Implicated in Intracellular Fusion – Rabs, Tethers and Phosphoinositide Lipids	64
C. Cell–Cell Fusion	65
1. Sperm–Egg Fusion	65
2. Myoblast Fusion	66
VI. Toward a Resolution of Membrane Fusion Mechanisms	66
VII. References	66

## I. Introduction

Specific fusion of biological membranes is a central requirement for many cellular processes.<sup>1</sup> Membrane fusion involves the merging of the membranes of two different organelles and the mixing of aqueous compartments encapsulated by these membranes. Studies of membrane fusion mechanism have extensively employed lipid vesicles as artificial “organelles” (see

section III). The general fusion reaction scheme is given by



where A and B are separate organelles or vesicles, AB is the “docked” prefusion complex, and C is the fused product (see Figure 1). The reaction may proceed spontaneously if the reactants are inherently unstable. For example, it is possible to produce small unilamellar lipid vesicles (approximately 20 nm in diameter) by ultrasonication, a process that introduces energy into the system. These vesicles possess a high degree of positive curvature on their outer monolayer and a high degree of negative curvature on their inner monolayer (see section III). If these vesicles are made of lipids that experience stress in these curved environments, they will spontaneously proceed to the fusion reaction. When the vesicles are metastable, only small perturbations (e.g., addition of divalent ions, polyethylene glycol, or peptides) are needed to drive the reaction.

Biological organelles or vesicles, on the other hand, are intrinsically stable; otherwise, they would wreak havoc inside the cell. Biological fusion events are strongly regulated and coordinated by specific “docking” and “fusion” proteins. The best-studied examples of these fusion proteins are viral envelope proteins (see section IV). More recently, proteins that mediate intracellular and extracellular fusion events have been identified and characterized (see section V). In biological systems, docking molecules are needed to associate potential fusion partners and fusion proteins are the catalysts that drive the reaction. In Figure 1, E represents the unmodified fusion protein, and E' is the protein modified as a result of the fusion reaction. In enzyme-catalyzed reactions, the protein frequently performs its catalytic function without modification of its structure. However, the action of fusion proteins is generally accompanied by large conformational changes that are irreversible in the case of viral fusion proteins. Intracellular fusion proteins have the capability of regenerating their original structure as indicated by the curved back arrow in Figure 1.

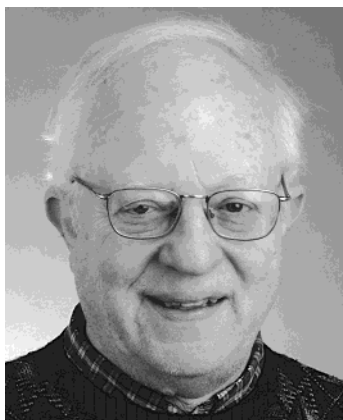
Along the fusion reaction pathway, a number of intermediate states have been identified. The analysis of the physical and thermodynamic parameters that govern these intermediate states has led to important insights regarding fusion mechanisms. These will be discussed in section III. In biological

\* To whom correspondence should be addressed at Center for Cancer Research, P.O. Box B, Bldg. 469, Rm. 216A, Miller Drive, Frederick, MD 21702-1201. Phone: 301 846-1446; FAX: 301 846-6192; e-mail: blumen@helix.nih.gov.

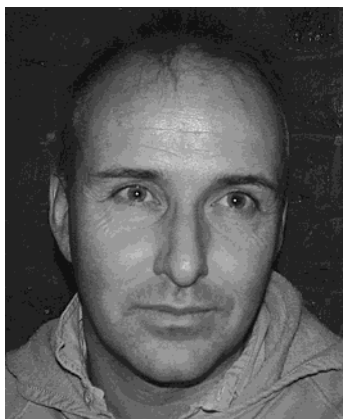
<sup>†</sup> Center for Cancer Research, National Cancer Institute, National Institutes of Health, Bethesda-Frederick, MD.

<sup>‡</sup> Physiological Laboratory, University of Liverpool, Crown St., Liverpool L69 3BX, UK.

<sup>§</sup> Department of Biochemistry, McMaster University, Hamilton, ON Canada L8N 3Z5.

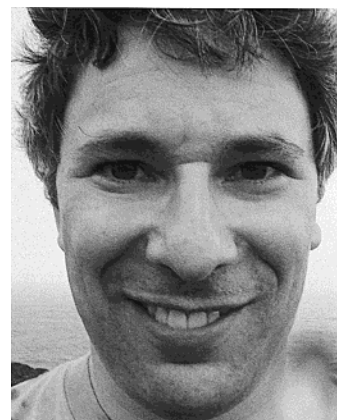


Dr. Blumenthal obtained his Ph.D. in physical chemistry at the Weizmann Institute. Following postdoctoral work at the Institute Pasteur and at Columbia University, he came to the National Institutes of Health (NIH) and was ultimately recruited by the National Cancer Institute. Dr. Blumenthal has been awarded a Senior Biomedical Research Scientist position by the NIH. He is head of Section on Membrane Structure and Function in the Center for Cancer Research, NCI-Frederick. Dr. Blumenthal has worked in a wide range of areas in membrane biophysics, which includes membrane fusion, membrane transport, cell surface receptors, immune cytotoxic mechanisms, and use of liposomes for delivery of drugs and genes into cells. He is associate editor of *Molecular Membrane Biology*. Dr. Blumenthal's current interest is in viral fusion and the cell biology of virus entry.

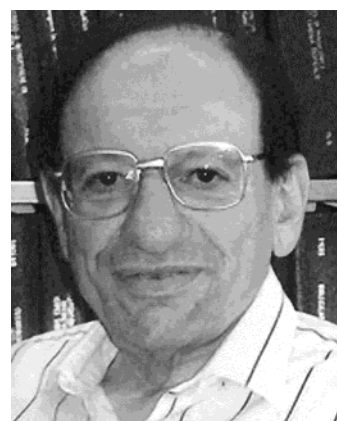


Michael J. Clague was born in Merseyside. He received his B.Sc. in Chemistry from the University of Exeter and his doctorate degree in biological chemistry from the University of Essex. He was a postdoctoral fellow at the National Cancer Institute, Bethesda and EMBL, Heidelberg. He is currently a Reader in Physiology at the University of Liverpool. He is interested in the regulation of cellular membrane traffic and phosphatidylinositol metabolism.

fusion processes, the reaction needs to be directed in a well-defined way. To provide a molecular interpretation of the sequence of events in the fusion reaction a plethora of mechanistic models have been invoked. These "fusion machines" contain building blocks that represent partially characterized protein structural motifs. In viral fusion, the "machines" are relatively simple since speed and fidelity of action are not of essence. In fusion processes that mediate synaptic transmission, speed and fidelity are essential and are reflected in the complexity of protein assembly. These processes form the basis of cognitive processes in higher organisms. In sections IV and V, we shall review the current knowledge regarding the *modus operandi* of the primitive and complex fusion machines, respectively.



Stewart Durell was born in Brooklyn, New York, and educated in Brooklyn Friends School and New York's City-As-School. He achieved a B.S. degree in biology from the State University of New York, College at Brockport, and a Ph.D. degree in biophysics from the Ohio State University. He is currently a staff scientist in the Laboratory of Computational and Experimental Biology, National Cancer Institute. His research concentrates on using computer methods to analyze and model membrane-bound and soluble proteins, with emphasis on identifying targets and developing drugs for medical purposes.



Richard M. Epand was born in New York City. He received his A.B. degree from the Johns Hopkins University and doctorate degree from Columbia University. He was postdoctoral fellow at Cornell University and visiting scientist at the Institute for Biochemical Research in Buenos Aires and at Yale University. Dr. Epand is currently Managing Editor of the journal *Chemistry and Physics of Lipids*. He is the recipient of the 1999 Avanti Award in Lipids and has been made a Fellow of the Biophysical Society. His research interests are in the area of membrane biophysics.

## II. Membrane Fusion Assays

The criterion for fusion of membranes is the merging of their lipid bilayer and cytoplasmic continuity (Figure 1). This leads to diffusion of the lipid molecules and intermixing of water-soluble substances bounded by the membranes. The majority of the assays for monitoring fusion are based on measuring intermixing of lipid or water-soluble molecules using a wide variety of biochemical and biophysical techniques. In addition, electron microscopy (EM) remains an important tool to visualize the fusion reaction. For instance, when lipid mixing assays are performed visualization by EM becomes crucial to distinguish whether lipid mixing indeed reports on fusion rather than on processes that involve the disintegration of fusing partners followed by rearrangements of their membranes.<sup>2,3</sup> However, the use of EM for studying mechanisms of fusion often

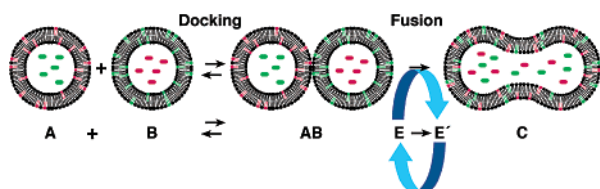


**Figure 1.** The membrane fusion reaction. Two lipid vesicles (A and B) form close contacts, “docking” (AB) and then proceed to become one vesicle (C). The mixing of lipid and aqueous markers originally in the separate vesicles (green and red) report on the progress of the fusion reaction. The reaction may proceed spontaneously (see section III) or via catalysis by specific proteins (see sections IV and V). These proteins may be involved in “docking” and fusion. In the latter case, a conformational transition of the catalyst ( $E \rightarrow E'$ ) is coupled to the transitions of the lipids.

becomes very challenging since fusion is a very rapid and localized phenomenon that involves molecular rearrangements of a relatively small number of molecules. Major problems are the possibility for artifacts due to the preparation of specimen, misinterpretations of the EM pictures, and difficulties in quantitation.<sup>4</sup> However, novel developments in cryo-electron microscopy of frozen hydrated samples in combination with image reconstruction<sup>5</sup> have provided crucial information regarding stages toward productive fusion of a virus with liposomes.<sup>6</sup> The virus studied in this context, Semliki forest virus, is particularly suited for these studies because of its icosahedral symmetry. Nevertheless, important information regarding the fusion of the less ordered influenza virus with liposomes<sup>7</sup> can be gleaned using this technique as described in section IV. In the case of cell membranes, recent improvements in both methods and instrumentation have led to the visualization of EM structures with 5–8-nm resolution.<sup>8</sup> Thanks to high-pressure freezing, cellular specimens of considerable size can now be well frozen, even without the addition of chemical cryoprotectants. With this and other methods for rapid freezing, samples become solidified within milliseconds whereupon they are embedded in glasslike ice. The cellular milieu is still aqueous, but rapid freezing has immobilized all the cell's constituents before significant rearrangement is possible. Under these conditions, biological structure is trapped in an essentially native state, and ice crystals, which would deform the physiological organization, have had little time to grow. In section IV, we shall discuss the use of transmission electron microscopy to image thin sections of rapidly frozen, freeze-substituted specimens of influenza hemagglutinin (HA)-mediated fusion.<sup>9</sup>

### A. Liposomes as Models

Studies of liposome fusion have provided a great deal of the background concerning the proper use of lipid probes and aqueous probes to study membrane fusion (for reviews, see volumes 220 and 221 in *Methods of Enzymology* (1993)). They have also provided a wealth of information on how the chemical and physical properties of lipids influence the fusion reaction.<sup>10</sup> Membrane fusion requires at least two distinct processes, binding or apposition of two

membranes and the subsequent merger of these membranes (see Figure 1). In the case of liposome fusion polyethylene glycol is a widely used agent that brings liposomes into juxtaposition (see section III). Peptides and proteins have also been used to promote aggregation of liposomes.<sup>4</sup> For analysis of the fusion reaction, the two processes must be dissociated either by prebinding the two fusion partners so that only the fusion rate is measured or by a kinetic analysis, such as the mass action model developed by Nir.<sup>11</sup> By performing such an analysis, it has been shown that potential fusogens may increase the overall fusion rate by causing enhancement of liposome aggregation without affecting the actual fusion step.

Figure 1 shows how fluorescent probes are used to monitor the merging of the membranes and the mixing of aqueous compartments encapsulated by these membranes. The rate of aggregation can be monitored by changes in light scattering.<sup>12</sup> The rate of fusion is monitored by changes in the fluorescence of lipid<sup>13</sup> or aqueous probes.<sup>14</sup> Redistribution of lipid probes can occur in the absence of the mixing of aqueous contents. This process termed “hemifusion”, in which only the two contacting (cis) monolayers combine, will be extensively discussed in section III.

Lentz and co-workers<sup>15,16</sup> have considerably expanded the repertoire of biophysical techniques to monitor the sequence of molecular events associated with PEG-induced fusion of liposomes. These events include: (1) vesicle aggregation measured by light scattering changes, (2) outer leaflet mixing by changes in the lifetime of a fluorescent lipid (DPHpPC) incorporated into the outer monolayer, (3) transfer of protons between the aqueous compartments of liposomes monitored by fluorescent changes of a fluorescent pH indicator, (4) inner leaflet mixing monitored by redistribution of a fluorescent lipid, (5) contents mixing monitored by fluorescence quenching assays. The sequence of molecular events suggested by these observations showed marked similarity to the sequence of viral and intracellular protein-mediated events that lead to fusion as shown by electrophysiological methods (see below).

A different geometry of fusing entities is provided by experiments that involve the fusion of liposomes with planar phospholipid bilayers.<sup>17</sup> This morphology corresponds to the fusion of secretory vesicles or of intact virus with plasma membranes of the cell. In a number of electrophysiological studies on the fusion of phospholipid vesicles to planar phospholipid membranes, fusion has been demonstrated by membrane mixing with incorporation of channels from the vesicular to the planar membrane and by aqueous content mixing seen with fluorescence.<sup>17</sup> In an elegant series of experiments, Chanturiya and co-workers<sup>17</sup> made simultaneous measurements of lipid dye mixing (membrane merger), aqueous dye mixing (content mixing), and electrical measurements of planar membrane conductance during the fusion of vesicles to planar bilayers. This way the time frame between mergers of membrane leaflets, the formation of the fusion pore, and the release of vesicular contents could be resolved. This report also demon-

strated flickering fusion pore formation (see below) between purely lipid bilayer membranes.

## B. Biological Membranes

A wide variety of “biological” membrane fusion assays have been developed that are tailored to the characteristics of the participating membranes. In the ideal assay binding would be resolved from fusion, and information on the kinetics and extent of fusion can be obtained.

### 1. Virus–Cell Fusion

The most popular and robust method of measuring virus fusion with target cells takes advantage of the large differential in surface area of the fusion partner membranes. The lipophilic dye octadecylrhodamine is initially incorporated into the viral membranes at self-quenching concentrations; fusion leads to dilution and hence an increase in fluorescence.<sup>18</sup> Several virus fusion proteins require a low pH environment to trigger the conformational changes necessary to elicit fusion (see section IV). In the natural course of events, this would be provided within endosomal compartments of target cells, but can also be provided artificially to cell-surface bound virions. In this case, it is possible to dissect virion-binding kinetics from fusion kinetics by carrying out a binding incubation at neutral pH (and 4 °C to inhibit endocytosis if necessary). Following removal of unbound virus, application of a low-pH fusion trigger is followed by a rise in fluorescence corresponding to membrane mixing that is normally monitored by a fluorimeter, although imaging of individual fusion events has been accomplished.<sup>19</sup> The red blood cell has proved a convenient target membrane for several of the more promiscuous viruses, e.g., influenza, VSV. In this case, there are no complications of the kinetics associated with endocytosis.

High resolution of the fusion kinetics can be obtained by employing stopped-flow mixing<sup>20,21</sup> or by decreasing the temperature.<sup>22,23</sup> Both approaches reveal a delay time between the low pH trigger and fluorescence dequenching which is associated with the progression through intermediate states of the fusion pathway (see section IV). Careful controls must be used for judging the specificity of the fluorophore transfer and the labeling protocol optimized accordingly.<sup>24</sup>

### 2. Cell–Cell Fusion Mediated by Viral Proteins

It has been recognized for some time that cell–cell fusion can occur as a result of virus cell interaction.<sup>25</sup> The fusion can be induced either after the virus fuses with the plasma membrane, or after biosynthesis and expression of the viral envelope protein on the cell surface. Gething and Sambrook<sup>26</sup> provided the first unambiguous assignment of a fusion protein by engineering cells to express influenza HA. This paper opened up new approaches to studying fusion events mediated by viral glycoproteins allowing site-directed mutagenesis studies<sup>27–29</sup> and the employment of techniques that take advantage of the large size of the expressing cells. In particular, the expressing

cells are amenable to patch clamping, which allows measurement of membrane capacitance (which is proportional to the membrane area of the patched cell) with millisecond time resolution.<sup>30</sup> Thus, triggered fusion with target cells, e.g., erythrocytes, is registered as a rise in capacitance. Electrophysiological measurements can also provide information on the evolution of conductance of the fusion pore.<sup>31,32</sup>

The flow of fluorescent marker between partner cells can also be monitored using modern imaging apparatus. This has allowed the simultaneous monitoring of the flux of membrane and cytoplasmic markers<sup>33,34</sup> and even in one case the differential transfer of inner and outer membrane lipids.<sup>35</sup>

### 3. Intracellular Fusion

The dissection of intracellular fusion events has been driven by both biochemistry and yeast genetics. Rothman and co-workers first established a biochemical assay that involves a specific intracellular fusion event by reconstituting transport between the cis and medial stacks of the Golgi.<sup>36</sup> They combined wild type Golgi fractions from CHO cells with Golgi from a clone lacking GlcNAc transferase activity, but containing VSVG protein by virtue of prior infection. Only by transfer between Golgi stacks could the VSVG protein acquire radiolabeled GlcNAc. They were able to show that this transfer required both cytosol and ATP and they embarked on a dissection of the cytosolic factors required to support the assay. A major insight derived from this work was that specificity of fusion is principally determined biochemically rather than relying on the architecture of the cell interior.

One drawback of this original assay was that it required generation of a vesicular intermediate, and essential factors could therefore operate at the level of vesicle budding, vesicle docking, or vesicle fusion. Assays that reconstitute other transport steps have since been established (see for example *Methods in Enzymology* volume 219). A heavily exploited one has been the homotypic fusion of early endosomes, which appears to reflect a direct fusion event without the generation of an intermediate vesicle.<sup>37,38</sup> A popular configuration of this assay involves the internalization of avidin or biotin-horseradish peroxidase into separate cell populations, isolation of endosomal fractions, and then combining in the presence of cytosol and salts. Contents mixing of endosomal lumens are assayed by quantitation of avidin–biotin complex formation.

A related, but more powerful assay combines this biochemical approach with yeast genetics. Homotypic fusion between isolated yeast vacuoles from different yeast strains is measured colorimetrically following the fusion of vacuoles containing pro-alkaline phosphatase, but lacking the protease required for cleavage and activation, with vacuoles containing the protease.<sup>39</sup> This has allowed the manipulation of membrane proteins in the assay by deletion of specific genes in the parent yeast strains, which enables the testing of the roles of individual proteins and the topological constraints for their participation in fusion<sup>40,41</sup> (see section V).

Weber et al. have developed an assay that reconstitutes intracellular fusion between liposomes using a minimal set of components, namely, the synaptic SNAREs described in section V.<sup>3</sup> They mimic the physiological situation by preparing a set of liposomes bearing the integral membrane protein synaptobrevin and a second set bearing the integral membrane protein syntaxin 1 complexed with SNAP-25. The first set of liposomes is labeled with fluorescent lipids that are subject to a concentration-dependent quenching of their emission. Upon fusion with unlabeled liposomes the lipid analogues are diluted, resulting in an increase in fluorescence that can be monitored as a function of time (see section IIA).

In the particular case of regulated exocytosis, highly resolved kinetic data has been obtained, due to a well-defined trigger (increase in cytosolic  $\text{Ca}^{2+}$ ) and the response time of the detection methods, e.g., patch clamp capacitance measurements or the use of amperometry to detect the localized release of catecholamines or neurotransmitters.<sup>42</sup>

### III. Membrane Rearrangements Required for Fusion

#### A. Adhesion, Deformation, and Fusion of Bilayers

The likelihood of surfaces coming in close contact has been estimated in the framework of the Derjaguin–Landau–Verwey–Overbeek (DLVO) theory.<sup>43</sup> This theory has been developed for aggregation of colloidal particles and considers the interplay of attractive van der Waals and repulsive electric double layer forces between charged surfaces in liquids. It allows calculation of the free energy of interaction between the particles,  $\Delta G$ , as a function of the separation distance between the surfaces,  $h$ . The ratio of the number of particles at a distance  $h$  to that at an infinite separation is given by the Boltzmann equation,  $\exp[-\Delta G(h)/kT]$ , where  $k$  is the Boltzmann constant and  $T$  is the absolute temperature. Stable association between two vesicles that are fusion partners occurs if  $\Delta G/kT \gg 1$  (Figure 1), i.e., the inter-membrane energy of interaction  $\Delta G$  should be sufficient to overcome the Brownian motion. Obviously, in biological systems (sections IV and V) specific “docking molecules” are used to achieve stable associations between potential fusion partners.

The DLVO theory fails to describe interactions between lipid bilayers at short separations (of the order of nanometers). By measuring changes in bilayer spacing in multilamellar vesicles as a function of externally applied osmotic or hydrostatic pressure, Parsegian, Rand and their collaborators discovered a surprisingly strong exponentially growing (characteristic decay length of 0.1–0.2 nm) repulsive force between phospholipid bilayers.<sup>44,45</sup> Insensitivity of this force to membrane electrostatics led to the initial conclusion that the repulsive force is due to hydration of the polar lipid headgroups by water. However, it is now generally believed that other forces also contribute to this repulsion including steric interactions<sup>46</sup> along with elastic pressures.<sup>47</sup> In addition, an attractive force between closely apposed membranes has been observed by measurements of adhesion of

bilayers supported on mica surfaces in aqueous solutions.<sup>48,49</sup> This force is believed to arise from exposure of hydrophobic moieties of phospholipids as a result of the stress exerted on the bilayer surfaces that approach within about 1 nm.

A theoretical analysis of interactions between apposed membranes puts forward the notion that out-of-plane thermal fluctuations of the bilayers lead to the formation of close (less than 0.5 nm) contact between the membranes within a small area (approximately 10 nm<sup>2</sup>).<sup>50</sup> According to this theory, increasing hydration repulsion between apposed polar heads of lipid molecules in this area causes the rupture of interacting monolayers. The rupture results in monolayer fusion of the membranes, i.e., in the formation of a bridge connecting the monolayers, which is usually named the stalk or hemifusion intermediate (see next section).

Poly(ethylene glycol) (PEG) has been widely used to study the parameters that govern membrane adhesion and fusion.<sup>51–53</sup> The threshold concentration of PEG required to induce the aggregation of phospholipid vesicles increases with a decrease in the molecular weight of PEG from 5% (w/w) with PEG 6000 to more than 30% (w/w) with PEG 200.<sup>52</sup> As two membranes approach, there will be less polymer between the membranes than in the bulk solution resulting in an osmotic gradient that will force the two surfaces together.<sup>51,52,54</sup> The nonadsorbing polymer may also promote lateral contraction of the membrane lipids leading to the exposure of more hydrophobic regions of the membrane.<sup>55</sup> Molecular dynamics simulations indicate that the close juxtaposition of two membranes results in the disorientation and exposure of the lipid acyl chains.<sup>56</sup> It is important that the polymers are excluded from the membrane surface since anchoring lipid-conjugated PEG to membranes will have the opposite effect.<sup>57,58</sup> There are diverse effects of polymers on membrane fusion that can be used to study the roles of both lipid hydration and the steric barrier in influencing the rate of membrane fusion. In addition, these polymers are of interest and importance in their own right. PEG is commonly used to induce cell–cell fusion to produce hybrids, while other polymers such as dextran sulfate may be developed into an antiviral agent.

#### B. Membrane Curvature and Destabilization

Monolayer curvature has been defined from the perspective of an observer in the hydrophobic interior of the bilayer looking out at the headgroups:<sup>59,60</sup> positive when concave, negative when convex. Negative intrinsic monolayer curvature is a property of lipids that are more stable when forming a curved structure with the phospholipid headgroups occupying a smaller cross sectional area than the ends of the acyl chains. It is generally thought that the lipid rearrangements during the fusion reaction proceed in at least two stages (Figure 2). In the first, the contacting monolayers (referred to as “cis”) leaflets have merged, but the distal (denoted “trans”) leaflets have remained intact. The structures of these intermediates have been described as “stalks” that further evolve to form a hemifusion diaphragm (Figure 2A).<sup>61</sup>

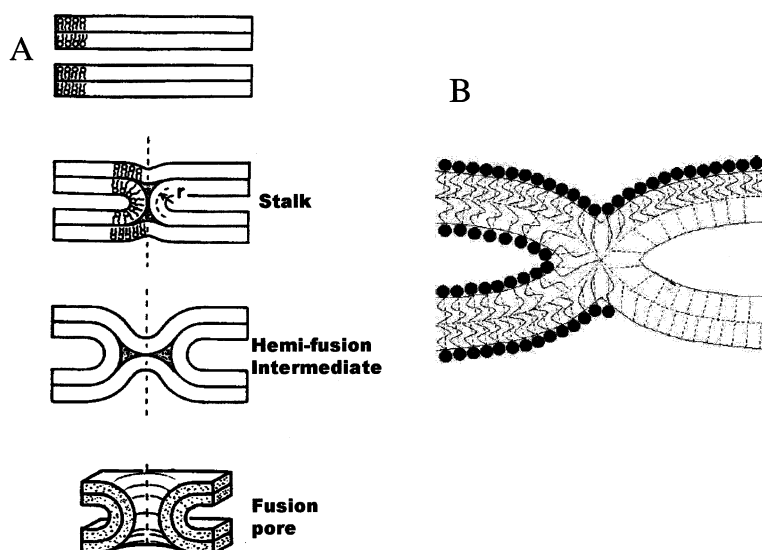


**Figure 2.** Schemes for membrane fusion. (A) Adapted from Figure 6 of ref 61 Siegel and Epanand with permission. Copyright 1997 Biophysical Society. Top drawing represents two juxtaposed bilayers before they begin to fuse. Stalk shows the intermediate with the contacting (cis) monolayers acquiring negative curvature with radius  $r$ . It should be noted that the negative curvature is clear in this side view; however, if the stalk intermediate is viewed from the top, then the curvature of the cis monolayer would be positive, particularly in the center of the stalk. A hemifusion intermediate results from the juxtaposition of the trans monolayers. The fusion pore is the first intermediate that can allow mixing of aqueous contents. (B) Adapted from Figure 2 of ref 65 Kozlovsky and Kozlov with permission. Copyright 2002 Biophysical Society. There are now no hydrocarbons packing voids, as represented by the stippled black areas in the stalk and hemifusion intermediates in section A.

The transmonolayers making up the hemifusion diaphragm then rupture to form the complete fusion pore.

The fusion intermediates are of course three-dimensional and the curvature properties are not the same in all dimensions. In the hemifusion intermediates, for example, the lipids of both the cis and trans monolayers acquire overall negative curvature.<sup>61</sup> However, the curvature is negative only in the dimension viewed in a cross-section of the bilayer (see Figure 2). The well-characterized lamellar-to-inverted hexagonal phase transitions seen in bulk lipids involve the formation of connections between adjacent bilayers. The formation of the stalk intermediate in membrane fusion also entails the formation of these connections. It has recently been shown that at a relative humidity in the range of 70 to 80%, diphtanoyl phosphatidylcholine forms a phase in which the lipid is arranged with hourglass-shaped structures,<sup>62</sup> similar to the morphology that has been suggested for the stalk (Figure 2). Previous estimations of the energetics of fusion were based on the formation of an inverted phase.<sup>63</sup> The availability of the X-ray structure of a stalk-like arrangement of lipid will allow for a more accurate calculation of the energetics of formation of this intermediate.

Lipids in a bilayer arrangement fill space uniformly. However, converting a flat bilayer to a fusion intermediate, in which one of the monolayers is curved, results in packing voids or it requires a range of tilts of the acyl chains. These are energy requiring processes. All other things being equal, any membrane fusion intermediate that minimizes distortions in phospholipid packing will be energetically favored. Comparing the bicontinuous cubic phase with the hexagonal phase, the former has fewer packing defects, but it also does not completely relieve cur-

vature stress.<sup>64</sup> A modified version of the hemifusion stalk intermediate has recently been proposed that deals with the energy crisis provided by these packing defects.<sup>65</sup> This model includes changes in acyl chain tilt in addition to bending of the monolayer. The model avoids having to fill hydrocarbon-packing voids (compare Figure 2A,B). In the earlier models of the stalk formation, the proposed structure had regions of lower density of lipid, resulting from the space left between the cis and trans monolayers forming as a consequence of the cis monolayer acquiring a greater degree of curvature. These packing voids had to be filled in by stretching of some acyl chains, a process requiring energy. The formation of these hydrocarbon packing voids are avoided in the model of Kozlovsky and Kozlov<sup>65</sup> (Figure 2). As a consequence, the energy of the stalk intermediate is lowered from approximately 150 kT in the model of Siegel to a value of less than 50 kT. The splay of the hydrocarbon chains produced by tilting at least partially compensates for the splay produced by monolayer bending. In addition, this model has the advantage that the overall area of the stalk monolayers is reduced compared with the earlier models. In this version of the stalk intermediate, the energetic barrier presented to the fusion process becomes much lower and more in line with what is required by experimental observation.<sup>65</sup> In fact, the model predicts that with membranes of certain spontaneous splay, fusion intermediates can be thermodynamically stable structures. The recent observations of a phase of phospholipid that contains the hourglass-shaped stalk structure<sup>62</sup> bear out this prediction.

The stalk intermediate is suggested to evolve into a fusion pore during the fusion event. The fusion pore has been compared with the connections between unit cells in a bicontinuous cubic phase. However, it

should be noted that the bicontinuous cubic phase has an average curvature of zero, while this is not the case for a fusion pore. This difference is difficult to reconcile using the approaches that have been applied up to now. The physics of bilayer fusion is severely complicated by the involvement of a broad range of length and time scales. Whereas the stability of vesicles can be understood from continuum models, the creation of the fusion pore occurs within a volume of a few nanometers (i.e., at atomic scales) and is generally assumed to proceed much faster than microseconds. Thus, for the critical transition steps during fusion, the finite size and the thermal fluctuations of the lipid molecules may be relevant, in which case simple continuum models would be insufficient. To describe such events, atomistic models will likely be required.<sup>66</sup>

The stalk-pore paradigm is supported by a large body of evidence showing that either viral fusion or the fusion of liposomes is facilitated by the presence of lipids in the cis monolayer that have large intrinsic negative monolayer curvature propensity. In addition, compounds that promote positive curvature inhibit viral fusion. One example is cholesterol hemisuccinate that inhibits fusion only at neutral pH where it promotes positive curvature, but not at acidic pH.<sup>67</sup> Similarly, inhibition is also observed with the addition of lysophosphatidylcholine (LPC) to the cis monolayer.<sup>68</sup> To complete the fusion process the trans-monolayer has to assume positive curvature (Figure 2A).<sup>68</sup> Evidence for this requirement has been established by showing that fusion pore formation is promoted by adding LPC to the trans monolayer side<sup>69</sup> and inhibited by adding negative curvature-promoting amphiphiles to the same side.<sup>70</sup>

Whatever mechanism drives the process forward, the essential role of fusion catalysts is to accelerate the rate of fusion, i.e., lower the activation energy for fusion. The destabilization of the lipid bilayer as a result of the interaction of segments of fusion proteins with membranes provides a way to lower these barriers. There have been many studies showing that synthetic peptides, which promote liposome fusion, are capable of destabilizing membrane bilayers.<sup>71</sup> One motif for destabilizing membranes that appears to be common to a number of diverse fusion systems, is for the entry of the peptide into the membrane as an  $\alpha$ -helix inserted at an oblique angle. This motif has been demonstrated by polarized FTIR on viral fusion peptides and has been shown to correlate with the fusogenic activity of the intact virus.<sup>72,73</sup> It should be pointed out, however, that modeling the membrane-inserted fusion peptide as a rigid  $\alpha$ -helix is likely to be an oversimplification. It has recently been shown that the fusion peptide of influenza virus inserts into a membrane in a distorted helix with a kinked structure.<sup>74</sup>

#### IV. Viral Membrane Fusion

Enveloped viruses have evolved different but conceptually related mechanisms to fuse their membranes with cellular membranes during entry into cells.<sup>75</sup> At least two different classes of viral fusion proteins can be distinguished.<sup>76</sup> Class I is represented

by orthomyxo-, retro-, paramyxo-, and filoviruses. Their fusion proteins mature by proteolytic cleavage of a precursor protein, yielding a membrane-anchored subunit with an amino-terminal or amino-proximal fusion peptide. Application of the fusion trigger (receptor binding or low pH) results in the formation of a characteristic trimeric postfusion structure with a triple-stranded coiled coil at its core.<sup>77,78</sup>

Representatives of class II include flavi- and alphaviruses. Their fusion proteins are not proteolytically cleaved and have internal rather than amino-terminal fusion peptides. They are synthesized as a complex with a second membrane glycoprotein, and the activation of the fusogenic potential involves the cleavage of this accessory protein.<sup>79</sup> X-ray crystallography of two class II fusion proteins, the E protein of the flavivirus tick-borne encephalitis virus<sup>80</sup> and the E1 protein of the alphavirus Semliki forest virus,<sup>6</sup> has revealed a common overall fold for these proteins, which are structurally unrelated to class I viral fusion proteins. Although some fascinating new features regarding fusion mechanisms are emerging as a result of these studies with class II fusion proteins, we will limit our discussion of viral envelope glycoprotein-mediated fusion to its prototype, influenza hemagglutinin (HA), a class I fusion protein whose structure and function have most extensively been studied.<sup>81</sup>

#### A. Structure of Native and Low pH Influenza Hemagglutinin (HA)

Influenza virus employs a complex cellular entry route that involves binding to cell surface receptors, endocytosis through clathrin-coated pits and vesicles, followed by delivery to a low pH endosomal compartment.<sup>82</sup> The triggering signal that leads to influenza virus fusion is relatively simple, requiring only low pH.<sup>81</sup> Other class I viruses, such as HIV, employ a more direct entry route; they fuse directly with the plasma membrane at neutral pH following the binding to cell surface receptors.<sup>83</sup> However, the triggering signals are more complicated in that they require receptor-induced conformational changes in viral envelope glycoproteins.<sup>84</sup>

HA is a trimeric integral membrane protein ( $M_r$  220 000) comprised of an ectodomain of identical subunits, each of which contains two polypeptides, HA1 and HA2, linked by a disulfide bond.<sup>85</sup> The two subunits arise from a proteolytic cleavage event that is essential for fusion activity.<sup>86</sup> HA1 is the receptor-binding subunit, and HA2 is responsible for the fusogenic activity of HA.<sup>81</sup>

Structural information is available for the ectodomains of both the native protein at neutral pH<sup>85</sup> and portions of HA2 following exposure to low pH<sup>87,88</sup> (see Figure 3). The HA trimer protrudes 130 Å from the viral membrane (Figure 3A). Each monomer is composed of two distinct regions, namely, a fibrous stem containing residues from HA1 and HA2, and a globular region composed solely of HA1 residues arranged in an eight-stranded  $\beta$ -structure.<sup>85</sup> A significant number of residues within the HA2 subunits adopt a triple-stranded  $\alpha$ -helical coiled-coil that stabilizes the HA trimeric structure. HA1 globular

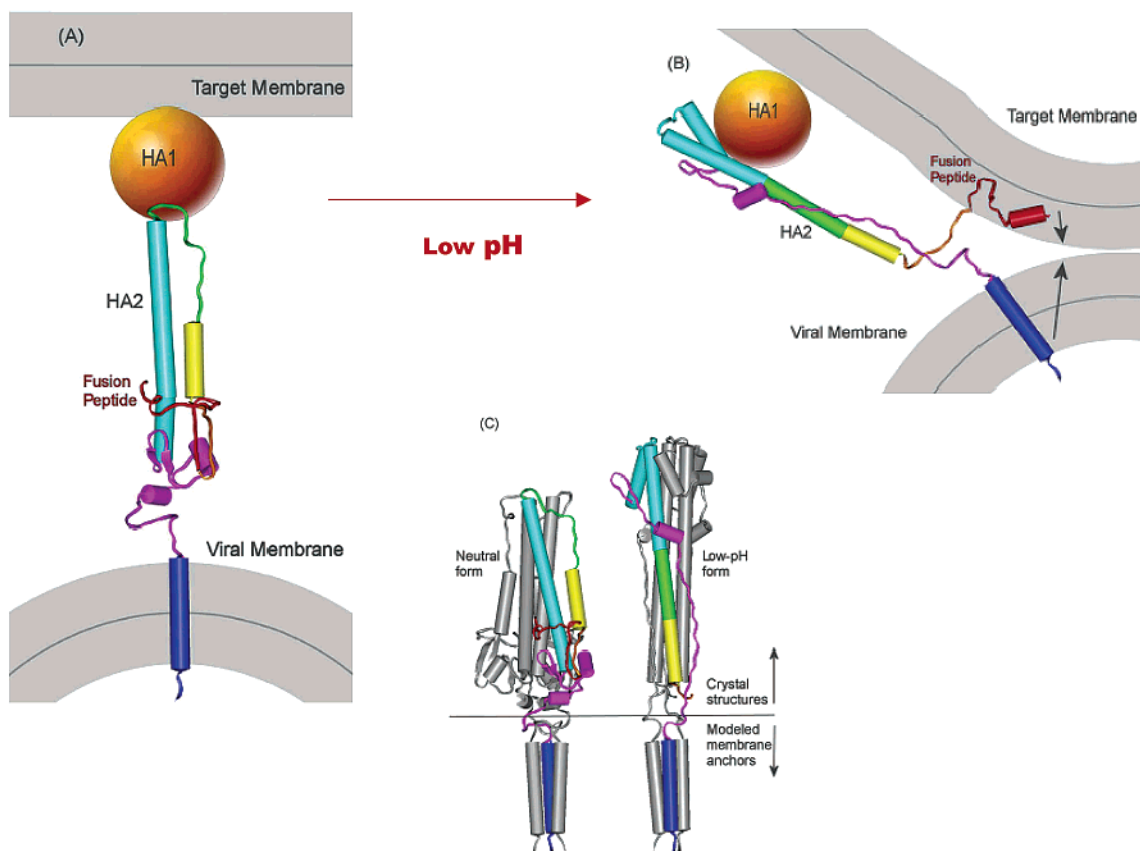


**Figure 3.** Model for membrane deformation catalyzed by influenza HA. The three panels contrast HA in the neutral<sup>85</sup> and low-pH<sup>88</sup> conformational forms. Where possible, the protein cartoons of HA2 were developed directly from crystal structure coordinates: i.e., residues 1–175 of 1HGG.pdb (neutral form) and residues 31–183 of 1QU1.pdb (low-pH form) from the Protein Data Bank.<sup>201</sup> The atomic models were completed by adding the membrane-bound fusion peptide structure obtained by Tamm et al.<sup>74</sup> to the N-terminal of the low-pH structure (residues 1–30, red), and connector residues and idealized helices to the C-terminals of both structures to form the viral membrane anchors (residues 186–215, blue). The models are consistent with the actual sequence of HA2, and represent the different protein segments in sterically feasible relative positions. To discern the details of the structural changes only one monomer of the protein trimer is shown in figures (A) and (B), and HA1 is simply represented as a sphere binding to the target membrane. (A) In the neutral form HA1 clamps HA2 into an  $\alpha$ -helix (residues 38–55, yellow)  $\leftrightarrow$  loop (residues 56–75, green)  $\leftrightarrow$   $\alpha$ -helix (residues 76–125, cyan) conformation. (B) Lowering the pH results in dissociation of HA1 from the core of the protein and four major changes in HA2: (i) The green loop adopts a helical conformation and residues 106–111 of the cyan helix convert to a loop conformation, effectively shifting the triple-stranded helical coiled-coil core (shown in C) of the protein toward the N-terminal. (ii) The C-terminal of the cyan helix (residues 112–128) becomes antiparallel to the new helical core (residues 37–105). (iii) The mixed-secondary-structure chain connecting the C-terminal cyan helix to the viral membrane anchor (residues 129–185, magenta) adopts a more extended conformation, with an approximate 4.5-fold increase in end-to-end distance (in this case from 21 to 96 Å). (iv) Residues 34–37 at the N-terminal and residues 174–176 of the extended C-terminal combine in the trimer to form an annular “N cap” at the N-terminal of the triple-stranded coiled-coil, which stabilizes the structure.<sup>88</sup> (C) Observing the trimeric-forms of HA2 illustrates how the extended C-terminal magenta and equivalent gray segments pack in the grooves between the three central coiled-coil helices of the low-pH form. The fusion peptides are not shown in the low pH form of Figure 3C. One subunit in each structure is color-coded as in parts (A) and (B) for comparison. These large-scale conformational changes result in the release of the fusion peptides from their packed positions in the neutral-form protein, which allows for insertion into the viral and/or target membranes. A small group of proximal HA2 molecules simultaneously inserted into both the viral and target membranes would then constitute a potential fusion site.<sup>99</sup> The combination of conformational changes and the stabilization of the low-pH structures generate the stresses in the viral and target membranes (indicated by arrows) that induce contact and fusion. See text for further details.

subunits also associate into a trimeric assembly, and the N and C terminal regions of HA1 participate in long-range interactions with HA2 in the stem region. The glycine-rich NH<sub>2</sub> terminal (residues 1–20) region of HA2 has been designated as the fusion peptide based on a variety of genetic, protein chemical, and biophysical studies.<sup>73,74</sup> In the native trimeric HA structure at neutral pH, the three fusion peptides adopt sequential reverse turn conformations and are partially buried between  $\alpha$ -helices at the interface between the HA2 and HA1 subunits, near the viral side of the ectodomain stalk (see Figure 3A). Activa-

tion of HA at low pH results in extensive molecular rearrangements leading to extrusion of the fusion peptide from this buried location, whereupon it can interact with the target and/or viral membrane.<sup>81</sup> This is a consequence of forming an extended coiled-coil conformation<sup>89</sup> (see Figure 3B). Determination of the HA structure in the activated, low-pH state has been hindered by the exposure of the hydrophobic fusion peptide, which causes disordered aggregation of the trimers in aqueous solution. However, the high-resolution structure of a stable truncated recombinant ectodomain of the fusion-pH conformation of



HA2, which lacks the N-terminal fusion peptide, has been determined at 1.9 Å resolution.<sup>88</sup> According to this structure, the N- and C-terminal residues of the molecule form an N cap, terminating both the N-terminal  $\alpha$ -helix and the central coiled-coil (Figure 3). Comparison with the crystal structures of a number of other membrane fusion-inducing proteins reveals common structural motifs,<sup>78</sup> which suggest potential mechanisms for membrane fusion.

## B. Conformational Changes in Influenza HA

Extensive studies have been performed on the acid-triggered conformational changes that are related to the fusogenic activity of influenza HA.<sup>90</sup> White and Wilson<sup>91</sup> have probed the details of the pH-dependent conformational changes in X31 HA using a panel of anti-HA-peptide antibodies. The results of their study indicate that the acid-triggered conformational change of isolated HA occurs in at least two steps: the fusion peptide comes out of the trimer interface ("intermediate state") followed by dissociation of the globular heads ("the low pH form"). The intermediates are also characterized by susceptibility to proteinase K digestion and binding to liposomes.<sup>92,93</sup> Although these intermediates may actually consist of a population of states, for convenience we will refer to these as the "intermediate state". Upon acidification to the optimal pH for fusogenic activity at 37 °C and pH 5.0, long-range contacts between HA1 interfaces are disrupted, as indicated by changes in spike morphology<sup>93–95</sup> and reactivity to anti-peptide antibodies raised against the top and interface regions.<sup>91</sup> Pretreatment of X31 virus under these conditions leads to inactivation of HA-mediated fusion. By contrast, in the intermediate state, HA maintains its spike morphology and fusogenic potential.<sup>94</sup> Recently, Herrmann and his group have calculated that the trimeric structure is loosened at low pH as a result of electrostatic repulsion.<sup>96</sup> Relief of this electrostatic repulsion could be the energy that is coupled to membrane fusion.

The widely accepted "spring-loaded" type of mechanistic models for HA-mediated fusion posit that the cleaved HA is a metastable intermediate in which extensive contacts between HA1 and HA2 kinetically trap the molecule behind a free-energy barrier.<sup>89</sup> Application of an acidic trigger surmounts the barrier to yield a stable low pH conformation of HA2.<sup>87</sup> Raising the temperature<sup>97</sup> or adding denaturants<sup>98</sup> can also bring about release of the spring-load. According to the "spring-loaded" model the most plausible scenario is that activation of the fusion protein results in release of the fusion peptide and extension of a central coiled-coil structure (Figure 3B). The new positioning of the fusion peptides at the tip of the stalk provides for easy contact with the target cell membrane. A small group of proximal fusion proteins that are simultaneously inserted into both the viral and target membranes would constitute a potential fusion site<sup>99</sup> (see Figure 3). Electron microscopy studies of antibody complexes of influenza virus haemagglutinin following low pH triggering support this mechanism.<sup>100</sup>

However, influenza HA-mediated fusion can take place while the bulk of the HA molecules appear to

be unaltered.<sup>7</sup> This observation would support the view that the fusion-active form is not significantly altered in three-dimensional structure from native HA<sup>22</sup> and that the low-pH state is in fact an endpoint in the pH-dependent structural changes.<sup>101,102</sup> Consistent with this model is the observation that fusion has been observed to occur under conditions that either precede, or where changes in HA shape are not detected, either by electron microscopy<sup>93–95,101,103</sup> or by using antibody probes.<sup>22</sup> Moreover, recent differential scanning calorimetric measurements show that unfolding of neutral pH HA is an endothermic process,<sup>104,105</sup> indicating that the whole molecule is not in a metastable high-energy state. Furthermore, in a recent study on the relationship between acid-induced changes in thermal stability and fusion activity of HA it was shown that X31 influenza virus retains its fusion activity at acidic pH at temperatures significantly below the unfolding transition of HA.<sup>104</sup>

The "spring-loaded" model, on the other hand, proposes that the conformational change, which involves the loop to helix transition of HA2 residues 56–75 (see Figure 3B),<sup>87,89</sup> is required for fusion. This model is supported by the observation that specific proline substitutions in this region that prevent formation of the low pH HA2 structure abolish HA fusion activity.<sup>106,107</sup> Moreover, the observation that introduction of intermonomer disulfide bonds impair HA fusion activity indicate that some separation of the globular head domains is required for X31 HA fusion.<sup>108,109</sup> The seemingly contradictory observations that viral particles composed of HA in its unfolded state can fuse, but that fusion requires structural rearrangement of HA can be reconciled by the notion that only a few HA molecules are involved in the fusion process.<sup>34,102,110,111</sup> It has recently been proposed that the few molecules in the contact site are sufficient to initiate fusion events that lead to redistribution of lipids, but that wide pore may require the involvement of a large number of fusion proteins outside the contact area.<sup>112</sup>

## C. The Influenza HA-Mediated Fusion Cascade

Kinetic fusion studies of fluorescently labeled virus and cells have been performed to dissect the events that occur following the low pH triggering of HA.<sup>113</sup> One of the interesting characteristics of the kinetics is the appearance of delays in lipid redistribution following low pH triggering, suggesting a multistep process.<sup>21</sup> By lowering the temperature, a long-lived low pH HA fusion intermediate has been identified that is committed to fusion.<sup>23</sup> Following a temperature jump to 37 °C at neutral pH this intermediate proceeds to fusion at a similar rate and extent as that seen for low pH fusion. The committed state is insensitive to treatments with trypsin or DTT, which release HA1, but is reversed by treatment with proteinase K and thermolysin, which affect HA2. The committed state thus represents interactions between HA2, presumably including the fusion peptide, and the target membrane. Comparative studies on commitment to fusion induced by wild-type HA and a

fusion peptide mutant HA indicate tight coupling between conformational changes in HA and fusion peptide insertion.<sup>114</sup> Chernomordik and co-workers have further characterized this state as a “restricted hemifusion” intermediate<sup>115,116</sup> that can be “frozen” at low temperatures. Video microscopy observations on single influenza virions fusing with RBC show that movement of lipid is restricted during the initial stages of fusion<sup>117</sup> and that lipid dispersal could occur without redistribution of HA from virus to cell.<sup>19</sup>

By employing simultaneous measurements of pairs of assays for fusion, the subsequent order of detectable events was determined:<sup>9,31,32,34,118</sup> A transient fusion pore then redistribution of lipid, followed by redistribution of small and large aqueous markers. The fact that redistribution of lipid dyes precedes that of aqueous markers is consistent with the notion that HA-catalyzed fusion can be described by the stalk–pore paradigm (see section III). The observation, on the other hand, that a transient fusion pore may precede outer monolayer continuity could be interpreted in terms of the proteinaceous fusion pore hypothesis.<sup>31,42</sup> However, the same fusion phenotypes including the transient fusion pore have been observed in the case of fusion between purely lipid bilayer membranes<sup>15,17</sup> Moreover, the observation that the lipid composition of the membranes can differentially augment or suppress HA-mediated fusion supports the stalk–lipidic pore concept.<sup>118</sup>

HA-mediated fusion thus proceeds through a hemifusion intermediate, which is defined as the merging of the contacting monolayers of two membranes without distal monolayer merger or fusion pore formation. The hypothesis is widely held that hemifusion is a key intermediate stage of membrane fusion.<sup>119</sup> This concept was further supported by the observation of stable lipid mixing intermediates induced by the glycosylphosphatidylinositol-linked ectodomain of HA, GPI–HA, lacking its transmembrane domain and cytoplasmic tail<sup>120</sup> as well as by certain replacements of the N-terminal residue of HA2.<sup>28,121</sup> However, a recent attempt to visualize the fine structure of the contact area between GPI–HA-expressing cells and RBC using transmission electron microscopy to image thin sections of rapidly frozen, freeze-substituted material did not reveal any such diaphragms with the limits of detection (70–100 nm).<sup>9</sup> Presumably, diaphragms need to be about an order of magnitude larger to be revealed by transmission electron microscopy. However, a multiplicity of small fusion sites was observed within which either lipid redistribution or fusion pore formation could ensue.<sup>9</sup> These contact sites appear in the form of dimples on both membranes. Such dimpling, which has previously been observed in the process of exocytosis in mast cells,<sup>122</sup> has been put forward as an early step in the fusion reaction.<sup>103,123–126</sup> Frolov et al.<sup>9</sup> observed these dimples in both GPI–HA and HA, indicating that the transmembrane domain may not be essential for contact site formation. However, agents that increase the positive curvature of inner monolayers promote fusion pore expansion in the GPI–HA hemifusion intermediate.<sup>127</sup> Therefore, it seems likely that the TM domain of intact HA

promotes fusion pore expansion by perturbing the inner monolayers of the fusing membranes.

The major challenge in the field is to understand how conformational changes in the fusion proteins drive the changes in lipid dispositions required for fusion. Figure 3 shows a model in its most rudimentary form for the coupling between structural changes in HA and deformation of the target and viral membranes. The models are thus consistent with the actual sequence of HA2, and thus represent the different protein segments in sterically feasible relative positions. A more extensive version that includes a number of steps has recently been presented by White and colleagues.<sup>107</sup> Lowering the pH (see Figure 3) results in dissociation of HA1 from the core of the protein and a number of drastic changes in HA2 that include (i) a loop to helix transition resulting in a new long helix (yellow–green–cyan) that forms an N-terminal triple-stranded coiled coil (see Figure 3C), (ii) a helix to loop (“kink”) transition in the cyan helix that results in an antiparallel reorientation of residues 112–128 to the new long core helix, (iii) an extension of the mixed-secondary-structure chain (magenta) that now binds to the groove between helices of the N-terminal coiled coil (see Figure 3C). The tension created by binding of these C-terminal extended regions into the grooves presumably provides the driving force needed to pull viral and target membranes together.<sup>107</sup>

According to the model shown in Figure 3, the conformational transitions in HA2 are coupled to deformation of the target and viral membranes through the fusion peptide and TM anchor, respectively. Although there appears to be wide latitude in the sequence of the TM domain that supports fusion,<sup>128</sup> mutations of the TM domain,<sup>120,129</sup> as well as of the fusion peptide<sup>28,121</sup> may produce unstable intermediates that give rise to lipid mixing and/or transient pores only. Only strong interactions of these crucial domains of the fusion proteins with the lipid membranes will ensure the completion of the reaction.

Several additional models have been proposed to describe the way conformational changes in the fusion proteins drive the changes in lipid dispositions. Kozlov and Chernomordik<sup>130</sup> have suggested a mechanism for the promotion of fusion by the influenza hemagglutinin protein (HA) in which a conformational change in the protein can cause local bending of the viral membrane, priming it for fusion. The fusion peptide is proposed to insert into the viral membrane. The subsequent refolding of the protein exerts a force on the fusion peptide that tends to bend the membrane around an HA trimer into a saddle-like shape. According to this model, low pH-induced aggregation of intact HA is driven by the elastic energy derived from the bending of the membrane around HA2 coiled-coil trimers into a saddle-like shape. Bulging of the viral membrane produces a dimple. Bending stresses on the lipidic top of the dimple facilitate membrane fusion. The model for HA aggregation-driven fusion is supported by data on lipid mixing mediated by a construct of HA2 consisting of amino acids 1–127, which include the fusion

peptide and the kink (residues 106–111, Figure 3) that presumably is responsible for the pH-driven aggregation of HA molecules.<sup>131–133</sup>

A related mechanism for defect formation was proposed by Bentz,<sup>102</sup> except that in this mechanism the conformational change in the protein is coupled with the formation of a defect in the membrane as a result of the withdrawal of the fusion peptide from the membrane, leaving a hydrophobic defect. A variation of the idea of the formation of a nipple, but in both fusing components, has been combined with the suggestion that there are small movements of the lipids out of the plane of the bilayer.<sup>126</sup>

## V. Cellular Fusion

### A. SNAREs

Within every cell, every minute, hundreds of membrane fusion and fission events take place. The net result of all this activity is the set of intracellular organelles with which we are familiar, such as the Golgi stacks, endosomes, and lysosomes. The fact that they retain their identities, in the face of so much membrane flux, implies that there must be a means by which fusion partners are restricted. The SNARE hypothesis was proposed in 1993 by Rothman and co-workers to explain the specificity of intracellular fusion events<sup>134</sup> and has proved to be essentially robust in the face of much critical analysis. It proposes that, the core of the fusion machinery is comprised of SNARE proteins that are localized to specific subcellular compartments; only cognate SNAREs on partner membranes can form a complex that promotes fusion.

The first SNARE complex to be characterized specifies synaptic vesicle fusion with the plasma membrane.<sup>135</sup> This interaction, which is believed to be characteristic of all SNARE complexes,<sup>136</sup> involves the formation of a parallel four helix bundle in which one helix is contributed by a vesicle associated SNARE (v-SNARE), synaptobrevin (VAMP-2), while the other three are contributed by SNAREs on the target membrane (t-SNAREs). In this case, two helices are provided by SNAP-25 and one by syntaxin 1.<sup>137,138</sup> Sequence analysis has shown that all SNAREs probably derive from a single ancestral gene that has been duplicated in the case of SNAP-25.<sup>139</sup>

The human genome contains 35 SNARE proteins while that of *Saccharomyces cerevisiae* contains 21.<sup>140</sup> A signature feature is the presence of conserved heptad repeats in their membrane proximal regions that interact to form the four-helix bundle. In common with coiled-coil structures of viral envelope glycoproteins<sup>78</sup> the residues at “a” and “d” positions contribute to the hydrophobic core interactions which stabilize the structure. The structure of the synaptic SNARE complex revealed the presence of an ionic layer at the center of the otherwise hydrophobic core of the SNARE complex.<sup>137</sup> Synaptobrevin contributes an arginine (R) residue to this layer while the three helices from SNAP-25 and syntaxin each contribute a glutamine residue (Q). These residues are highly conserved, an observation that has led to a revised nomenclature for the SNAREs from the original t-

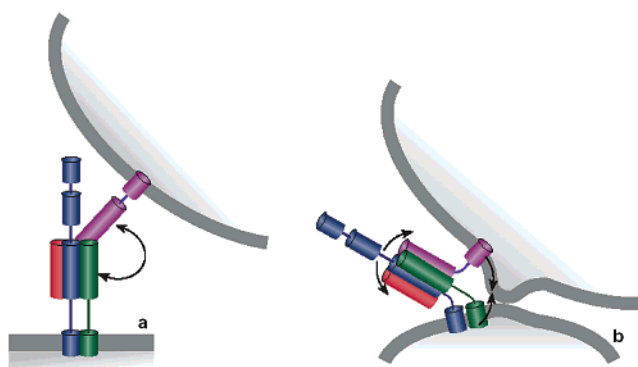


**Figure 4.** Model for membrane deformation mediated by SNARE proteins. (a) The four helical sections of SNARE proteins in a prefusion state arranged in a 3:1 distribution between partner membranes. Pink, v-SNARE, or R-SNARE; blue, syntaxin family member; red and green represent both light chains that are Q-SNAREs (in the neuronal SNARE complex, they are two chains of SNAP-25, but in the generalized form they may come from distinct proteins). (b) Progressive zipping of the four helical sections of SNARE proteins leads to the assembly of a tight parallel four-helix bundle. This process forces membranes into close membrane apposition and will generate stresses at the membrane that are coupled to imposed bending of the participating proteins (indicated by arrows).

and v-SNAREs to Q- and R-SNAREs.<sup>141</sup> It has been proposed that this layer may enforce the correct register during SNARE complex assembly<sup>136</sup> or effective coupling of ATPase hydrolysis of NSF to SNARE complex disassembly.<sup>142</sup>

The resolution of the SNARE complex structure immediately suggested an attractive mechanism by which it might promote fusion that has been termed “the zipper model” (see Figure 4). This mode of action would then be quite similar to that mediated by influenza HA (see Figure 3). In this model, the assembly of the parallel four-helix bundle occurs initially at the N-termini of the helices and zips up toward the membrane anchors, consequently pulling the partner membranes into close apposition.<sup>143</sup> The SNAREs themselves must tilt toward the membrane during this process, and it is attractive to speculate that this is coupled to deformation of the membrane through the transmembrane anchor. Insertion of a flexible linker between the transmembrane domain and the coiled-coil domain reduces SNARE-dependent fusion efficiency systematically with increasing length of the linker.<sup>144</sup> Note that after fusion, a SNARE complex will persist, but now in a *cis*-configuration until it is disassembled by the action of NSF, an ATPase.<sup>134</sup>

Evidence that SNAREs participate in a late stage of physiological fusion reactions has been provided by an assay of regulated secretion of dense core vesicles in PC12 cells. In this system, the assembly of the SNARE complex occurred after the rise in  $\text{Ca}^{2+}$  and could not be experimentally dissociated from the fusion process.<sup>145</sup> This same assay can be inhibited by addition of a soluble SNARE coiled-coil domain. Titration of this domain and fitting of the experimental data have suggested that three SNARE complexes cooperate to promote fusion.<sup>146</sup> In adrenal chromaffin cells, an antibody that inhibits SNARE assembly also reduces the initial fast component of

exocytosis indicating that even the vesicles poised for the quickest release require the SNARE assembly step.<sup>147</sup> Studies of embryonic neuronal cultures derived from synaptobrevin knockout mice have confirmed previous results from worms and flies, in that  $\text{Ca}^{2+}$  evoked neurotransmitter release is inhibited 100 fold, while spontaneous release of neurotransmitter is less sensitive, but nevertheless still reduced by 90%.<sup>148</sup>

The finding that the three synaptic SNAREs when distributed between liposomes in accord with cell physiology could promote liposome fusion led to the proposal that the SNAREpin complex represented the minimal fusion machinery.<sup>3</sup> This remains a controversial finding. The crux of the matter is to what extent does the “slow” fusion seen in this liposome based assay represent the actual biological fusion which can occur on the millisecond time-scale in the case of synaptic vesicle exocytosis.<sup>149</sup> There is little dispute that this assay is able to recapitulate a major physiological mechanism for imposing specificity of membrane recognition, but could the subsequent fusion be an artifact of the assay? It has been argued that the fusion observed is a nonspecific result of prolonged apposition between the partner membranes. One observation that argues against this is that substitution of the transmembrane domains of syntaxin and synaptobrevin with lipid anchors allows the docking interaction of vesicles to proceed, but fusion is no longer observed.<sup>150</sup> This is presumably because the formation of the helical bundle, which requires bending of the constituent proteins toward the membrane, is not effectively coupled to perturbation of the lipid bilayer.<sup>150</sup> Strikingly, a similar result is found in a more physiological system. Grote et al. have replaced the transmembrane domains of two exocytic SNAREs in yeast Snc2p and Sso2p with signals for a geranylgeranyl lipid anchor.<sup>151</sup> These SNAREs are correctly targeted and able to engage in SNARE complex assembly, but when overexpressed lead to inhibition of exocytosis after vesicle docking. This block to secretion occurs at a lipid sensitive stage of the fusion pathway as it can be partially reversed by adding lysoPC to the external leaflet of the plasma membrane that will endow it with positive curvature. This scenario is very similar to the GPI-HA paradigm<sup>120,127</sup> discussed in the previous section.

A cell free assay of yeast vacuole fusion (see section IIB), although it requires trans-SNARE complex formation,<sup>40</sup> provides the focus for questioning the notion that this complex provides the agonist for bilayer mixing. Clever manipulations of the assay allow its dissection into kinetically and biochemically defined steps. In one experiment the authors are ostensibly able to dissociate trans-SNARE complexes prior to fusion with excess NSF while nevertheless observing subsequent progression to fusion with normal kinetics.<sup>41</sup> One is struck here by the parallel with the “fusion committed” state induced by viral proteins described above. Could it be that SNAREs initiate the fusion reaction up to a point similar to that induced by influenza HA at low temperature? Presumably further energetic input is required to

complete the pathway efficiently. Set against this experiment are data from Weber et al. which demonstrate that in distinction to *cis*-SNARE complexes NSF is apparently unable to disassemble *trans*-SNARE complexes.<sup>152</sup>

Peters and colleagues have identified three factors downstream of trans-SNARE formation necessary for vacuolar fusion; release of  $\text{Ca}^{2+}$  from the vesicle lumen, calmodulin, and protein phosphatase 1.<sup>153,154</sup> The requirement for a specific SNARE combination is universal to all intracellular fusions. The requirement for vesicular calcium release and calmodulin is shared by assays of both early and late endosome fusion and of intra-Golgi transport in mammalian cell free systems.<sup>155–157</sup> A search for calmodulin binding partners on the vacuolar membrane using chemical cross linking identified the V0 sector of the vacuolar-ATPase<sup>158</sup> which is made up from Vma6, Vph1 and the proteolipids Vma3 (six copies), Vma11, and Vma16.<sup>159</sup> Intriguingly, these authors found that reconstituted V0 proteolipids could respond to  $\text{Ca}^{2+}$ /calmodulin by forming a channel permeable to entrapped choline; furthermore, trans-complexes of V0 were shown to form, after SNARE-dependent docking of vacuoles. The authors offer the challenging speculation that this trans-V0 complex evolves under the influence of  $\text{Ca}^{2+}$ /calmodulin to become the fusion pore that dilates by radial expansion and dissociation of the proteolipid ring.

The universality of the protein pore mechanism can be called into question, SNARE deletions in yeast are often lethal but yeast can grow in the absence of Vma3 in acidic media,<sup>159</sup> neither has the distribution of V0 throughout the cell been established. It may be that other proteins/proteolipids can fulfill this function; the authors point to Got1p and Sft2p that are small hydrophobic membrane proteins that are known to genetically interact with the Golgi SNARE Sed5p.<sup>160a</sup> However, recent observations on insulin secretion from intact mouse pancreas by two-photon excitation imaging indicate that the opening of the fusion pore was preceded by unrestricted lateral diffusion of lipids along the inner wall of the pore.<sup>160b</sup> These observations support the notion that this structure is composed of membrane lipids.

## B. Other Factors Implicated in Intracellular Fusion – Rabs, Tethers, and Phosphoinositide Lipids

Shuffling of SNARE combinations in the liposome assay has served to vividly demonstrate their capacity to impart specificity to vesicle fusion reactions.<sup>161</sup> However, SNAREs are not the whole story; it is now widely accepted that prior to SNARE complex assembly intracellular vesicles engage in foreplay through specific tethering molecules that contain long stretches of coiled-coil domain.<sup>162</sup> The key to describing these tethering activities is the development of assays that dissociate vesicle attachment from fusion.

EEA1 is required for homotypic endosome fusion.<sup>163</sup> It binds to membranes due to a 2-fold interaction with the lipid PtdIns3P and with rab5-GTP.<sup>164</sup> Christoforidis et al. used a fluorescence microscopic assay of endosomal vesicle clustering, in the presence of a

fusion block imposed by a dominant negative form of  $\alpha$ -SNAP (a protein that cooperates with NSF to disassemble cis-SNARE complexes), to demonstrate that EEA1 was a necessary and sufficient cytosolic factor to support this reaction.<sup>165</sup>

Cao et al. developed a simple centrifugation assay for vesicle attachment on the yeast ER-to-Golgi transport pathway.<sup>166</sup> They found that vesicle attachment could still be observed with strains carrying loss of function mutations of SNARE proteins. Vesicle association was found to require the cytosolic "tether" Uso1 and the small GTPase Ypt1, a member of the Rab family.

In both the above cases, Rab proteins are implicated in recruitment of tethers to target membranes. This is also the case for a family of large complexes, of which the prototype is the exocyst,<sup>167,168</sup> that are implicated in specific vesicle tethering events (reviewed in refs 169 and 170).

In the simplest model consistent with current data,<sup>171</sup> a rab family member in the GTP bound form recruits an extended coiled-coil tethering protein to one or both interacting membranes. The tether molecule then promotes attachment between vesicles for a time limited by the rate of rab nucleotide hydrolysis. If a *trans*-SNARE complex is able to form during this period, then irreversible SNARE-dependent steps on the fusion pathway can proceed. This provides for a kinetic proofreading mechanism superimposed on the innate specificity of SNARE interactions. The reality is likely to be far more complex owing to numerous other interactions that both rabs and tethers can engage in. For example, the endosome fusion regulator rab5 interacts with 21 proteins by affinity chromatography<sup>165</sup> while an associated tether molecule, EEA1 interacts both with SNARE proteins and with calmodulin.<sup>155</sup>

The role of lipids in vesicular transport processes has received much interest in recent years, with particular attention being given to phosphatidylinositol species. The six-carbon ring structure of the inositol headgroup provides a substrate that is utilized by specific kinases for phosphate addition at positions 3,4 and 5 on the ring. This can create up to eight different PtdIns lipid species within a cell which are put to a variety of uses, that include organization of the cytoskeleton and control of cell proliferation and survival pathways.<sup>172</sup> With regard to intracellular membrane fusion both PtdInsI(4,5) $P_2$  and PtdIns3 $P$  have well-established roles on the secretory and endocytic pathways, respectively. In neither case is that role a function of biophysical properties of the lipid bilayer associated with concentration of the above lipids. The lipids serve as identifiers of compartments and contribute to recruitment of proteins with specific binding domains to the endoplasmic surface of membranes. They may also act as allosteric regulators, but this has not been formally shown.

Permeabilized cell assays of regulated secretion in PC12 and chromaffin cells have revealed a requirement for PtdIns(4,5) $P_2$  generation by the consecutive action of PtdIns4-kinase and PtdIns(4 $P$ )5-kinase.<sup>173</sup> Several proteins implicated in this event have been shown to bind PtdIns(4,5) $P_2$  including calcium-de-

pendent activator protein for secretion (CAPS), Munc-18/Sec1 interacting proteins (MINTs), rabphilin, and synaptotagmin.<sup>174-177</sup>

Homotypic fusion of early endosomes requires PtdIns 3-kinase activity as judged by sensitivity to pharmacological inhibitors.<sup>178,179</sup> This requirement reflects recruitment of the tether molecule EEA1 to membranes through a specific interaction of its FYVE domain with PtdIns3 $P$ , which is concentrated on early endosomes.<sup>163,164,180</sup> Recruitment of EEA1 to endosomes can also be accomplished by binding to rab5, and, accordingly, at very high concentrations, rab5 can substitute for PtdIns 3-kinase activity.<sup>179,181</sup>

Monoclonal antibodies directed against PtdIns-(4,5) $P_2$  and its precursor PtdIns4 $P$  were found to inhibit yeast vacuole fusion, as did neomycin, a much less specific reagent that binds to inositol-polyphosphates.<sup>182</sup> By using two-stage incubations Mayer et al. could show that the final requirement for PI(4,5) $P_2$  lies somewhere between docking and the final stages of fusion, which are promoted by release of intravesicular calcium. An earlier requirement for PI(4,5)- $P_2$  on the fusion pathway could also be resolved that corresponds to a so-called "priming reaction" which precedes vesicle docking. Interestingly, the SNAP-25 homologue, t-SNARE molecule Vam7p, which participates in vacuolar fusion, is a mobile element of the SNARE complex that can be recruited to docking sites from the cytosol.<sup>183</sup> This is achieved through specific interaction of vacuolar PtdIns3 $P$  with its N-terminal PX domain.<sup>183,184</sup>

There are several hundred proteins in the human genome that contain phospho-phosphoinositide binding domains (e.g., FYVE, PX, PH, and ENTH domains). It is to be expected that more "fusion factors" utilizing this form of membrane association will be identified.

## C. Cell-Cell Fusion

Fusion events between cells play key roles in development, starting with fusion between sperm and egg and including myoblast fusion to form the myotubes that make up skeletal muscle. In each case, there has been a concerted effort to identify the fusion proteins, but little mechanistic data exist.

### 1. Sperm-Egg Fusion

Fertilization of eggs by mammalian sperm includes a complex set of steps that fall outside the scope of this review (reviewed by Wassarman<sup>185</sup>). Notably, sperm fusion competence requires the acrosome reaction, a specialized form of intracellular fusion involving a large secretory vesicle with the plasma membrane. However, we will confine our discussion to the final fusion event, that between sperm and egg membranes. Attention has focused on one particular sperm surface glycoprotein, fertilin, which is a heterodimer of  $\alpha$  and  $\beta$  N-glycosylated subunits, both of which are members of the ADAM family (*a* disintegrin and metalloprotease) of transmembrane proteins.<sup>186,187</sup> Both are synthesized as precursors by spermatogenic cells and are proteolytically processed to the mature form by removal of pro- and metalloprotease domains). Fertilin  $\beta$ -/- sperm show greatly

reduced ability to bind to the egg membrane.<sup>188</sup> Chen et al.<sup>189</sup> have suggested that high avidity interactions between fertilin  $\beta$  and an integrin ( $\alpha 6\beta 1$ ) on the egg plasma membrane requires cooperation between  $\alpha 6\beta 1$  and CD9, a protein that belongs to the tetraspan superfamily (TM4SF). CD9 knockout mice have shown an essential role for this protein in determining female fertility while otherwise presenting a normal phenotype.<sup>190–192</sup> Eggs are able to bind sperm normally but cannot subsequently fuse. On the other hand gamete fusion is unhindered in integrin  $\alpha 6\beta 1$  knockout mice.<sup>193</sup> Curiously, cellular expression of CD9 has also been shown to enhance membrane fusion and infection by canine distemper virus<sup>194</sup> and feline immunodeficiency virus.<sup>195</sup>

## 2. Myoblast Fusion

Skeletal muscle cells are multinucleate and formed through the aggregation and fusion of myoblasts. In vivo studies of muscle development in *Drosophila melanogaster* that combine ultrastructural observation with sophisticated genetics have led to the identification of candidate fusion proteins (reviewed by Taylor<sup>196</sup>).

In *Drosophila*, two classes of myoblasts form from the mesoderm, “founder cells” and fusion competent cells. Founder cells seed the muscles and impart specific characteristics to the muscle which forms following fusion with the second class of myoblasts. Apparently, each class of myoblast cannot fuse with themselves.

In *Drosophila* embryos with a small chromosomal deletion that includes the *dumbfounded* (*duf*) gene, no myoblast fusion occurs and no clusters of myoblasts form around the founders.<sup>197</sup> Mutations in another gene, *sticks and stones* (*sns*), that is expressed in the fusogenic myoblasts but not in founders also leads to failure of myoblast fusion.<sup>198</sup> Both *duf* and *sns* contain transmembrane domains and extracellular immunoglobulin-like repeats characteristic of the immunoglobulin superfamily of cell-adhesion molecules. It remains to be established if a direct *duf-sns* association promotes fusion and whether these molecules participate in the actual fusion event. The conservation of the *duf/sns* mechanism to mammalian cells is presently unclear, particularly as the closest mammalian homologue, nephrin functions in the kidney.<sup>198</sup> Recently, Podbilewicz and co-workers identified a gene in *C. elegans*, *eff-1*, which encodes a novel integral membrane protein that presumably mediates cell fusion.<sup>198a</sup>

Muscle derived mammalian cell lines will form myotubes in culture. Here, there are some intriguing parallels to sperm–egg fusion. Yagami-Hiromasa et al. have shown that meltrin- $\alpha$ , a homologue of fertilin, is associated with early stages of myotube formation.<sup>199</sup> Furthermore, antibodies against CD9 or CD81 delay fusion of C2C12 myoblast cells and RD rhabdomyosarcoma cells, while overexpression of CD9 promotes cell fusion in transfected myoblast-derived RD cell lines.<sup>200</sup> One is tempted to speculate that a conserved mechanism for cell–cell fusion utilizing tetraspanin proteins may exist.

## VI. Toward a Resolution of Membrane Fusion Mechanisms

The study of the chemistry and physics of lipids has provided a firm experimental and theoretical basis for understanding the forces governing close apposition between bilayer membranes. The subsequent events leading to bilayer fusion has been fit into a generally accepted conceptual framework, the stalk–pore hypothesis. However, the molecular details underlying the formation of these intermediate structures are subject to extensive debate. The very act of fusion in biological systems involves fast (microsecond to millisecond) molecular rearrangements of a small number (several to several hundred) of molecules. Although molecules outside the fusion contact region may indirectly affect the outcome of the fusion reaction,<sup>55,112</sup> the majority of the membrane molecules do not participate. Moreover, individual fusion events occur in a fairly random fashion. Therefore, from an experimental point, the capture of intermediate structures in the fusion reaction remains a daunting problem. Structures of intermediates have been inferred by calculations of the energy of putative intermediates as well as in experimental approaches. In addition, indirect evidence about the nature of fusion intermediates has been acquired by comparing the physical chemical properties of pure hydrated lipids in bulk with their effect on the outcome of the fusion reaction and by analyzing the various steps (e.g., mixing of monolayers, pore formation) that are components of the fusion reaction.

Significant advances have been made in the identification and elucidation of structures of proteins that catalyze membrane fusion. Experimental data indicate that protein-catalyzed fusion is governed by similar physical chemical principles as pure bilayer fusion. The main task of these protein catalysts is to provide specificity to the reaction by limiting it in time and space within the cells and to reduce the energy barriers for the pivotal stages of membrane coalescence and pore formation. Further understanding of the physical forces that drive lipids to undergo drastic transitions, and how conformational changes in proteins may be coupled to these transitions will provide insights into the modus operandi of biological fusion machines.

## VII. References

- (1) Blumenthal, R.; Dimitrov, D. S. *Handbook of Physiology*; Oxford University Press: New York, 1997; Chapter 14, pp 563–603.
- (2) Rand, R. P.; Kachar, B.; Reese, T. S. *Biophys. J.* **1985**, *47*, 483–489.
- (3) Weber, T.; Zemelman, B. V.; McNew, J. A.; Westermann, B.; Gmachl, M.; Parlati, F.; Sollner, T. H.; Rothman, J. E. *Cell* **1998**, *92*, 759–772.
- (4) Blumenthal, R. *Curr. Top. Membr. Transp.* **1987**, *29*, 203–254.
- (5) Baker, T. S.; Olson, N. H.; Fuller, S. D. *Microbiol. Mol. Biol. Rev.* **1999**, *63*, 862–922, table.
- (6) Lescar, J.; Roussel, A.; Wien, M. W.; Navaza, J.; Fuller, S. D.; Wengler, G.; Wengler, G.; Rey, F. A. *Cell* **2001**, *105*, 137–148.
- (7) Booy, F. *Viral Fusion Mechanisms*; CRC Press: Boca Raton, 1993; Chapter 2, pp 21–54.
- (8) McIntosh, J. R. *J. Cell Biol.* **2001**, *153*, F25–32.
- (9) Frolov, V. A.; Cho, M. S.; Bronk, P.; Reese, T. S.; Zimmerberg, J. *Traffic* **2000**, *1*, 622–630.
- (10) Haque, M. E.; McIntosh, T. J.; Lentz, B. R. *Biochemistry* **2001**, *40*, 4340–4348.
- (11) Nir, S. *Methods Enzymol.* **1993**, *220*: 379–91, 379–391.

- (12) Morris, S. J.; Bradley, D.; Gibson, G. C.; Smith, P. D.; Blumenthal, R. *Spectroscopic Membrane Probes*, CRC Press: Boca Raton, FL, 1988; Chapter 7, pp 161–191.
- (13) Hoekstra, D.; Duzgunes, N. *Methods Enzymol.* **1993**, *220*, 15–32.
- (14) Duzgunes, N.; Wilschut, J. *Methods Enzymol.* **1993**, *220*, 3–14.
- (15) Lentz, B. R.; Lee, J. K. *Mol. Membr. Biol.* **1999**, *16*, 279–296.
- (16) Lee, J.; Lentz, B. R. *Biochemistry* **1997**, *36*, 6251–6259.
- (17) Chanturiya, A.; Chernomordik, L. V.; Zimmerberg, J. *Proc. Natl. Acad. Sci. U.S.A.* **1997**, *94*, 14423–14428.
- (18) Hoekstra, D.; de Boer, T.; Klappe, K.; Wilschut, J. *Biochemistry* **1984**, *23*, 5675–5681.
- (19) Lowy, R. J.; Sarkar, D. P.; Whitnall, M. H.; Blumenthal, R. *Exp. Cell Res.* **1995**, *216*, 411–421.
- (20) Clague, M. J.; Schoch, C.; Zech, L.; Blumenthal, R. *Biochemistry* **1990**, *29*, 1303–1308.
- (21) Clague, M. J.; Schoch, C.; Blumenthal, R. *J. Virol.* **1991**, *65*, 2402–2407.
- (22) Stegmann, T.; White, J. M.; Helenius, A. *EMBO J.* **1990**, *9*, 4231–4241.
- (23) Schoch, C.; Blumenthal, R.; Clague, M. J. *FEBS Lett.* **1992**, *311*, 221–225.
- (24) (a) Stegmann, T.; Schoen, P.; Bron, R.; Wey, J.; Bartoldus, I.; Ortiz, A.; Nieva, J. L.; Wilschut, J. *Biochemistry* **1993**, *32*, 11330–11337. (b) Blumenthal, R.; Gallo, S. A.; Viard, M.; Raviv, Y.; Puri, A. *Chem. Phys. Lipids* **2002**, *116*, 39–55.
- (25) White, J.; Matlin, K.; Helenius, A. *J. Cell Biol.* **1981**, *89*, 674–679.
- (26) Gething, M. J.; Sambrook, J. *Nature* **1981**, *293*, 620–625.
- (27) Gething, M. J.; Doms, R. W.; York, D.; White, J. *J. Cell Biol.* **1986**, *102*, 11–23.
- (28) Schoch, C.; Blumenthal, R. *J. Biol. Chem.* **1993**, *268*, 9267–9274.
- (29) Lamb, R. A. *Virology* **1993**, *197*, 1–11.
- (30) Spruce, A. E.; Iwata, A.; White, J. M.; Almers, W. *Nature* **1989**, *342*, 555–558.
- (31) Tse, F. W.; Iwata, A.; Almers, W. *J. Cell Biol.* **1993**, *121*, 543–552.
- (32) Zimmerberg, J.; Blumenthal, R.; Sarkar, D. P.; Curran, M.; Morris, S. J. *J. Cell Biol.* **1994**, *127*, 1885–1894.
- (33) Sarkar, D. P.; Morris, S. J.; Eidelman, O.; Zimmerberg, J.; Blumenthal, R. *J. Cell Biol.* **1989**, *109*, 113–122.
- (34) Blumenthal, R.; Sarkar, D. P.; Durell, S.; Howard, D. E.; Morris, S. J. *J. Cell Biol.* **1996**, *135*, 63–71.
- (35) Nussler, F.; Clague, M. J.; Herrmann, A. *Biophys. J.* **1997**, *73*, 2280–2291.
- (36) Balch, W. E.; Dunphy, W. G.; Braell, W. A.; Rothman, J. E. *Cell* **1984**, *39*, 405–416.
- (37) Braell, W. A. *Proc. Natl. Acad. Sci. U.S.A.* **1987**, *84*, 1137–1141.
- (38) Gruenberg, J. E.; Howell, K. E. *EMBO J.* **1986**, *5*, 3091–3101.
- (39) Haas, A.; Wickner, W. *EMBO J.* **1996**, *15*, 3296–3305.
- (40) Nichols, B. J.; Ungermann, C.; Pelham, H. R.; Wickner, W. T.; Haas, A. *Nature* **1997**, *387*, 199–202.
- (41) Ungermann, C.; Sato, K.; Wickner, W. *Nature* **1998**, *396*, 543–548.
- (42) Lindau, M.; Almers, W. *Curr. Opin. Cell Biol.* **1995**, *7*, 509–517.
- (43) Verwey, E. J. W.; Overbeek, T. H. G. *Theory of Stability of Lyophobic Colloids*; Elsevier: Amsterdam, 1948.
- (44) Parsegian, V. A.; Fuller, N.; Rand, R. P. *Proc. Natl. Acad. Sci. U.S.A.* **1979**, *76*, 2750–2754.
- (45) Leikin, S.; Parsegian, V. A.; Rau, D. C.; Rand, R. P. *Annu. Rev. Phys. Chem.* **1993**, *44*, 369–395.
- (46) McIntosh, T. J.; Magid, A. D.; Simon, S. A. *Biochemistry* **1987**, *26*, 7325–7332.
- (47) Ito, T.; Yamazaki, M.; Ohnishi, S. *Biochemistry* **1989**, *28*, 5626–5630.
- (48) Helm, C. A.; Israelachvili, J. N.; McGuiggan, P. M. *Science* **1989**, *246*, 919–922.
- (49) Helm, C. A.; Israelachvili, J. N.; McGuiggan, P. M. *Biochemistry* **1992**, *31*, 1794–1805.
- (50) Leikin, S. L.; Kozlov, M. M.; Chernomordik, L. V.; Markin, V. S.; Chizmadzhev, Y. A. *J. Theor. Biol.* **1987**, *129*, 411–425.
- (51) Arnold, K.; Pratsch, L.; Gawrisch, K. *Biochim. Biophys. Acta* **1983**, *728*, 121–128.
- (52) Yamazaki, M.; Ohnishi, S.; Ito, T. *Biochemistry* **1989**, *28*, 3710–3715.
- (53) Burgess, S. W.; McIntosh, T. J.; Lentz, B. R. *Biochemistry* **1992**, *31*, 2653–2661.
- (54) Kuhl, T.; Guo, Y.; Alderfer, J. A.; Berman, A.; Leckband, D.; Israelachvili, J. N.; Hui, S. W. *Langmuir* **1996**, *12*, 3003–3014.
- (55) Safran, S. A.; Kuhl, T. L.; Israelachvili, J. N. *Biophys. J.* **2001**, *81*, 659–666.
- (56) Ohta-Iino, S.; Pasenkiewicz-Gierula, M.; Takaoka, Y.; Miyagawa, H.; Kitamura, K.; Kusumi, A. *Biophys. J.* **2001**, *81*, 217–224.
- (57) Basanez, G.; Goni, F. M.; Alonso, A. *FEBS Lett.* **1997**, *411*, 281–286.
- (58) Chams, V.; Bonnafous, P.; Stegmann, T. *FEBS Lett.* **1999**, *448*, 28–32.
- (59) Zimmerberg, J. *Traffic* **2000**, *1*, 366–368.
- (60) Gruner, S. M. *Proc. Natl. Acad. Sci. U.S.A.* **1985**, *82*, 3665–3669.
- (61) Siegel, D. P.; Epand, R. M. *Biophys. J.* **1997**, *73*, 3089–3111.
- (62) Yang, L.; Huang, H. W. *Science* **2002**, *297*, 1877–1879.
- (63) Siegel, D. P. *Biophys. J.* **1993**, *65*, 2124–2140.
- (64) Anderson, D. M.; Gruner, S. M.; Leibler, S. *Proc. Natl. Acad. Sci. U.S.A.* **1988**, *85*, 5364–5368.
- (65) Kozlovsky, Y.; Kozlov, M. M. *Biophys. J.* **2002**, *82*, 882–895.
- (66) Jahn, R.; Grubmuller, H. *Curr. Opin. Cell Biol.* **2002**, *14*, 488–495.
- (67) Cheetham, J. J.; Nir, S.; Johnson, E.; Flanagan, T. D.; Epand, R. M. *J. Biol. Chem.* **1994**, *269*, 5467–5472.
- (68) Chernomordik, L.; Kozlov, M. M.; Zimmerberg, J. *J. Membr. Biol.* **1995**, *146*, 1–14.
- (69) Chernomordik, L.; Chanturiya, A.; Green, J.; Zimmerberg, J. *Biophys. J.* **1995**, *69*, 922–929.
- (70) Razinkov, V. I.; Melikyan, G. B.; Epand, R. M.; Epand, R. F.; Cohen, F. S. *J. Gen. Physiol.* **1998**, *112*, 409–422.
- (71) Epand, R. M. *Biochim. Biophys. Acta* **1998**, *1376*, 353–368.
- (72) Horth, M.; Lambrecht, B.; Khim, M. C.; Bex, F.; Thiriart, C.; Ruyschaert, J. M.; Burny, A.; Bresseur, R. *EMBO J.* **1991**, *10*, 2747–2755.
- (73) Durell, S. R.; Martin, I.; Ruyschaert, J. M.; Shai, Y.; Blumenthal, R. *Mol. Membr. Biol.* **1997**, *14*, 97–112.
- (74) Han, X.; Bushweller, J. H.; Cafiso, D. S.; Tamm, L. K. *Nat. Struct. Biol.* **2001**, *8*, 715–720.
- (75) Hernandez, L. D.; Hoffman, L. R.; Wolfsberg, T. G.; White, J. M. *Annu. Rev. Cell Dev. Biol.* **1996**, *12*, 627–661.
- (76) Stiasny, K.; Allison, S. L.; Schalich, J.; Heinz, F. X. *J. Virol.* **2002**, *76*, 3784–3790.
- (77) Chan, D. C.; Kim, P. S. *Cell* **1998**, *93*, 681–684.
- (78) Skehel, J. J.; Wiley, D. C. *Cell* **1998**, *95*, 871–874.
- (79) Kielian, M.; Chatterjee, P. K.; Gibbons, D. L.; Lu, Y. E. *Subcell. Biochem.* **2000**, *34*: 409–55, 409–455.
- (80) Rey, F. A.; Heinz, F. X.; Mandl, C.; Kunz, C.; Harrison, S. C. *Nature* **1995**, *375*, 291–298.
- (81) Skehel, J. J.; Wiley, D. C. *Annu. Rev. Biochem.* **2000**, *69*, 531–569.
- (82) Marsh, M.; Helenius, A. *Adv. Virus Res.* **1989**, *36*, 107–151.
- (83) Moore, J. P.; Jameson, B. A.; Weiss, R. A.; Sattentau, Q. J. *Viral fusion mechanisms*; CRC Press: Boca Raton, 1993; pp 233–289.
- (84) Wyatt, R.; Sodroski, J. *Science* **1998**, *280*, 1884–1888.
- (85) Wilson, I. A.; Skehel, J. J.; Wiley, D. C. *Nature* **1981**, *289*, 366–373.
- (86) Klenk, H. D.; Rott, R.; Orlich, M.; Blodorn, J. *Virology* **1975**, *68*, 426–439.
- (87) Bullough, P. A.; Hughson, F. M.; Skehel, J. J.; Wiley, D. C. *Nature* **1994**, *371*, 37–43.
- (88) Chen, J.; Skehel, J. J.; Wiley, D. C. *Proc. Natl. Acad. Sci. U.S.A.* **1999**, *96*, 8967–8972.
- (89) Carr, C. M.; Kim, P. S. *Cell* **1993**, *73*, 823–832.
- (90) Wiley, D. C.; Skehel, J. J. *Annu. Rev. Biochem.* **1987**, *56*: 365–394.
- (91) White, J. M.; Wilson, I. A. *J. Cell Biol.* **1987**, *105*, 2887–2896.
- (92) Doms, R. W.; Helenius, A.; White, J. *J. Biol. Chem.* **1985**, *260*, 2973–2981.
- (93) Puri, A.; Booy, F.; Doms, R. W.; White, J. M.; Blumenthal, R. *J. Virol.* **1990**, *64*, 3824–3832.
- (94) Korte, T.; Ludwig, K.; Booy, F. P.; Blumenthal, R.; Herrmann, A. *J. Virol.* **1999**, *73*, 4567–4574.
- (95) Stegmann, T.; Booy, F. P.; Wilschut, J. *J. Biol. Chem.* **1987**, *262*, 17744–17749.
- (96) Huang, Q.; Opitz, R.; Knapp, E. W.; Herrmann, A. *Biophys. J.* **2002**, *82*, 1050–1058.
- (97) Ruigrok, R. W.; Martin, S. R.; Wharton, S. A.; Skehel, J. J.; Bayley, P. M.; Wiley, D. C. *Virology* **1986**, *155*, 484–497.
- (98) Carr, C. M.; Chaudhry, C.; Kim, P. S. *Proc. Natl. Acad. Sci. U.S.A.* **1997**, *94*, 14306–14313.
- (99) Weissenhorn, W.; Dessen, A.; Calder, L. J.; Harrison, S. C.; Skehel, J. J.; Wiley, D. C. *Mol. Membr. Biol.* **1999**, *16*, 3–9.
- (100) Wharton, S. A.; Calder, L. J.; Ruigrok, R. W.; Skehel, J. J.; Steinhauer, D. A.; Wiley, D. C. *EMBO J.* **1995**, *14*, 240–246.
- (101) Shangquan, T.; Siegel, D. P.; Lear, J. D.; Axelsen, P. H.; Alford, D.; Bentz, J. *Biophys. J.* **1998**, *74*, 54–62.
- (102) Bentz, J. *Biophys. J.* **2000**, *78*, 886–900.
- (103) Kanaseki, T.; Kawasaki, K.; Murata, M.; Ikeuchi, Y.; Ohnishi, S. *J. Cell Biol.* **1997**, *137*, 1041–1056.
- (104) Remeta, D. P.; Krumbiegel, M.; Minetti, C. A. S. A.; Puri, A.; Ginsburg, A.; Blumenthal, R. *Biochemistry* **2002**, *41*, 2044–2054.
- (105) Epand, R. M.; Epand, R. F. *Biochem. J.* **2002**, *365*, 841–848.
- (106) Qiao, H.; Pelletier, S. L.; Hoffman, L.; Hacker, J.; Armstrong, R. T.; White, J. M. *J. Cell Biol.* **1998**, *141*, 1335–1347.
- (107) Gruenke, J. A.; Armstrong, R. T.; Newcomb, W. W.; Brown, J. C.; White, J. M. *J. Virol.* **2002**, *76*, 4456–4466.
- (108) Godley, L.; Pfeifer, J.; Steinhauer, D.; Ely, B.; Shaw, G.; Kaufmann, R.; Suchanek, E.; Pabo, C.; Skehel, J. J.; Wiley, D. C. *Cell* **1992**, *68*, 635–645.
- (109) Kemble, G. W.; Bodian, D. L.; Rose, J.; Wilson, I. A.; White, J. M. *J. Virol.* **1992**, *66*, 4940–4950.

- (110) Danieli, T.; Pelletier, S. L.; Henis, Y. I.; White, J. M. *J. Cell Biol.* **1996**, *133*, 559–569.
- (111) Gunther-Ausborn, S.; Schoen, P.; Bartoldus, I.; Wilschut, J.; Stegmann, T. *J. Virol.* **2000**, *74*, 2714–2720.
- (112) Kozlov, M. M.; Chernomordik, L. V. *Traffic* **2002**, *3*, 256–267.
- (113) Blumenthal, R.; Schoch, C.; Puri, A.; Clague, M. J. *Ann. N. Y. Acad. Sci.* **1991**, *635*, 285–96, 285–296.
- (114) Korte, T.; Epand, R. F.; Epand, R. M.; Blumenthal, R. *Virology* **2001**, *289*, 353–361.
- (115) Chernomordik, L. V.; Leikina, E.; Kozlov, M. M.; Frolov, V. A.; Zimmerberg, J. *Mol. Membr. Biol.* **1999**, *16*, 33–42.
- (116) Leikina, E.; Chernomordik, L. V. *Mol. Biol. Cell* **2000**, *11*, 2359–2371.
- (117) Lowy, R. J.; Sarkar, D. P.; Chen, Y.; Blumenthal, R. *Proc. Natl. Acad. Sci. U.S.A.* **1990**, *87*, 1850–1854.
- (118) Chernomordik, L. V.; Frolov, V. A.; Leikina, E.; Bronk, P.; Zimmerberg, J. *J. Cell Biol.* **1998**, *140*, 1369–1382.
- (119) Palade, G. E. *Science* **1975**, *189*, 347–358.
- (120) Kemble, G. W.; Danieli, T.; White, J. M. *Cell* **1994**, *76*, 383–391.
- (121) Qiao, H.; Armstrong, R. T.; Melikyan, G. B.; Cohen, F. S.; White, J. M. *Mol. Biol. Cell* **1999**, *10*, 2759–2769.
- (122) Chandler, D. E.; Heuser, J. E. *J. Cell Biol.* **1980**, *86*, 666–674.
- (123) Monck, J. R.; Fernandez, J. M. *J. Cell Biol.* **1992**, *119*, 1395–1404.
- (124) Blumenthal, R.; Pak, C. C.; Raviv, Y.; Krumbiegel, M.; Bergelson, L. D.; Morris, S. J.; Lowy, R. J. *Mol. Membr. Biol.* **1995**, *12*, 135–142.
- (125) Lentz, B. R.; Malinin, V.; Haque, M. E.; Evans, K. *Curr. Opin. Struct. Biol.* **2000**, *10*, 607–615.
- (126) Kuzmin, P. I.; Zimmerberg, J.; Chizmadzhev, Y. A.; Cohen, F. S. *Proc. Natl. Acad. Sci. U.S.A.* **2001**, *98*, 7235–7240.
- (127) Melikyan, G. B.; Brenner, S. A.; Ok, D. C.; Cohen, F. S. *J. Cell Biol.* **1997**, *136*, 995–1005.
- (128) Melikyan, G. B.; Lin, S.; Roth, M. G.; Cohen, F. S. *Mol. Biol. Cell* **1999**, *10*, 1821–1836.
- (129) Armstrong, R. T.; Kushnir, A. S.; White, J. M. *J. Cell Biol.* **2000**, *151*, 425–437.
- (130) Kozlov, M. M.; Chernomordik, L. V. *Biophys. J.* **1998**, *75*, 1384–1396.
- (131) Epand, R. F.; Macosko, J. C.; Russell, C. J.; Shin, Y. K.; Epand, R. M. *J. Mol. Biol.* **1999**, *286*, 489–503.
- (132) Leikina, E.; LeDuc, D. L.; Macosko, J. C.; Epand, R.; Epand, R.; Shin, Y. K.; Chernomordik, L. V. *Biochemistry* **2001**, *40*, 8378–8386.
- (133) Epand, R. F.; Yip, C. M.; Chernomordik, L. V.; LeDuc, D. L.; Shin, Y. K.; Epand, R. M. *Biochim. Biophys. Acta* **2001**, *1513*, 167–175.
- (134) Sollner, T.; Bennett, M. K.; Whiteheart, S. W.; Scheller, R. H.; Rothman, J. E. *Cell* **1993**, *75*, 409–418.
- (135) Sollner, T.; Rothman, J. E. *Trends Neurosci.* **1994**, *17*, 344–348.
- (136) Chen, Y. A.; Scheller, R. H. *Nat. Rev. Mol. Cell Biol.* **2001**, *2*, 98–106.
- (137) Sutton, R. B.; Fasshauer, D.; Jahn, R.; Brunger, A. T. *Nature* **1998**, *395*, 347–353.
- (138) Poirier, M. A.; Xiao, W.; Macosko, J. C.; Chan, C.; Shin, Y. K.; Bennett, M. K. *Nat. Struct. Biol.* **1998**, *5*, 765–769.
- (139) Weimbs, T.; Mostov, K.; Low, S. H.; Hofmann, K. *Trends Cell Biol.* **1998**, *8*, 260–262.
- (140) Bock, J. B.; Matern, H. T.; Peden, A. A.; Scheller, R. H. *Nature* **2001**, *409*, 839–841.
- (141) Fasshauer, D.; Sutton, R. B.; Brunger, A. T.; Jahn, R. *Proc. Natl. Acad. Sci. U.S.A.* **1998**, *95*, 15781–15786.
- (142) Scales, S. J.; Yoo, B. Y.; Scheller, R. H. *Proc. Natl. Acad. Sci. U.S.A.* **2001**, *98*, 14262–14267.
- (143) Hanson, P. I.; Roth, R.; Morisaki, H.; Jahn, R.; Heuser, J. E. *Cell* **1997**, *90*, 523–535.
- (144) McNew, J. A.; Weber, T.; Engelman, D. M.; Sollner, T. H.; Rothman, J. E. *Mol. Cell* **1999**, *4*, 415–421.
- (145) Chen, Y. A.; Scales, S. J.; Patel, S. M.; Doung, Y. C.; Scheller, R. H. *Cell* **1999**, *97*, 165–174.
- (146) Hua, Y.; Scheller, R. H. *Proc. Natl. Acad. Sci. U.S.A.* **2001**, *98*, 8065–8070.
- (147) Xu, T.; Rammner, B.; Margittai, M.; Artalejo, A. R.; Neher, E.; Jahn, R. *Cell* **1999**, *99*, 713–722.
- (148) Schoch, S.; Deak, F.; Konigstorfer, A.; Mozhayeva, M.; Sara, Y.; Sudhof, T. C.; Kavalali, E. T. *Science* **2001**, *294*, 1117–1122.
- (149) Mayer, A. *Curr. Opin. Cell Biol.* **1999**, *11*, 447–452.
- (150) McNew, J. A.; Weber, T.; Parlatti, F.; Johnston, R. J.; Melia, T. J.; Sollner, T. H.; Rothman, J. E. *J. Cell Biol.* **2000**, *150*, 105–117.
- (151) Grote, E.; Baba, M.; Ohsumi, Y.; Novick, P. J. *J. Cell Biol.* **2000**, *151*, 453–466.
- (152) Weber, T.; Parlatti, F.; McNew, J. A.; Johnston, R. J.; Westermann, B.; Sollner, T. H.; Rothman, J. E. *J. Cell Biol.* **2000**, *149*, 1063–1072.
- (153) Peters, C.; Andrews, P. D.; Stark, M. J.; Cesaro-Tadic, S.; Glatz, A.; Podtelejnikov, A.; Mann, M.; Mayer, A. *Science* **1999**, *285*, 1084–1087.
- (154) Peters, C.; Mayer, A. *Nature* **1998**, *396*, 575–580.
- (155) Mills, I. G.; Urbe, S.; Clague, M. J. *J. Cell Sci.* **2001**, *114*, 1959–1965.
- (156) Porat, A.; Elazar, Z. *J. Biol. Chem.* **2000**, *275*, 29233–29237.
- (157) Pryor, P. R.; Mullock, B. M.; Bright, N. A.; Gray, S. R.; Luzio, J. P. *J. Cell Biol.* **2000**, *149*, 1053–1062.
- (158) Peters, C.; Bayer, M. J.; Buhler, S.; Andersen, J. S.; Mann, M.; Mayer, A. *Nature* **2001**, *409*, 581–588.
- (159) Stevens, T. H.; Forgac, M. *Annu. Rev. Cell Dev. Biol.* **1997**, *13*, 779–808, 779–808.
- (160) (a) Conchon, S.; Cao, X.; Barlowe, C.; Pelham, H. R. *EMBO J.* **1999**, *18*, 3934–3946. (b) Takahashi, N.; Kishimoto, T.; Nemoto, T.; Kadowaki, T.; Kasai, H. *Science* **2002**, *297*, 1349–1352.
- (161) McNew, J. A.; Parlatti, F.; Fukuda, R.; Johnston, R. J.; Paz, K.; Paumet, F.; Sollner, T. H.; Rothman, J. E. *Nature* **2000**, *407*, 153–159.
- (162) Pfeffer, S. R. *Nat. Cell Biol.* **1999**, *1*, E17–E22.
- (163) Mills, I. G.; Jones, A. T.; Clague, M. J. *Curr. Biol.* **1998**, *8*, 881–884.
- (164) Simonsen, A.; Lippe, R.; Christoforidis, S.; Gaullier, J. M.; Brech, A.; Callaghan, J.; Toh, B. H.; Murphy, C.; Zerial, M.; Stenmark, H. *Nature* **1998**, *394*, 494–498.
- (165) Christoforidis, S.; McBride, H. M.; Burgoyne, R. D.; Zerial, M. *Nature* **1999**, *397*, 621–625.
- (166) Cao, X.; Ballew, N.; Barlowe, C. *EMBO J.* **1998**, *17*, 2156–2165.
- (167) Hsu, S. C.; Ting, A. E.; Hazuka, C. D.; Davanger, S.; Kenny, J. W.; Kee, Y.; Scheller, R. H. *Neuron* **1996**, *17*, 1209–1219.
- (168) TerBush, D. R.; Maurice, T.; Roth, D.; Novick, P. *EMBO J.* **1996**, *15*, 6483–6494.
- (169) Short, B.; Barr, F. A. *Curr. Biol.* **2002**, *12*, R18–R20.
- (170) Whyte, J. R.; Munro, S. *J. Cell Sci.* **2002**, *115*, 2627–2637.
- (171) Clague, M. J. *Curr. Biol.* **1999**, *9*, R258–R260.
- (172) Fruman, D. A.; Meyers, R. E.; Cantley, L. C. *Annu. Rev. Biochem.* **1998**, *67*, 481–507, 481–507.
- (173) Martin, T. F. *Annu. Rev. Cell Dev. Biol.* **1998**, *14*: 231–64, 231–264.
- (174) Chung, S. H.; Song, W. J.; Kim, K.; Bednarski, J. J.; Chen, J.; Prestwich, G. D.; Holz, R. W. *J. Biol. Chem.* **1998**, *273*, 10240–10248.
- (175) Loyet, K. M.; Kowalchuk, J. A.; Chaudhary, A.; Chen, J.; Prestwich, G. D.; Martin, T. F. *J. Biol. Chem.* **1998**, *273*, 8337–8343.
- (176) Okamoto, M.; Sudhof, T. C. *J. Biol. Chem.* **1997**, *272*, 31459–31464.
- (177) Schiavo, G.; Gmachl, M. J.; Stenbeck, G.; Sollner, T. H.; Rothman, J. E. *Nature* **1995**, *378*, 733–736.
- (178) Jones, A. T.; Clague, M. J. *Biochem. J.* **1995**, *311*, 31–34.
- (179) Li, G.; D'Souza-Schorey, C.; Barbieri, M. A.; Roberts, R. L.; Klippel, A.; Williams, L. T.; Stahl, P. D. *Proc. Natl. Acad. Sci. U.S.A.* **1995**, *92*, 10207–10211.
- (180) Gillooly, D. J.; Morrow, I. C.; Lindsay, M.; Gould, R.; Bryant, N. J.; Gaullier, J. M.; Parton, R. G.; Stenmark, H. *EMBO J.* **2000**, *19*, 4577–4588.
- (181) Jones, A. T.; Mills, I. G.; Scheidig, A. J.; Alexandrov, K.; Clague, M. J. *Mol. Biol. Cell* **1998**, *9*, 323–332.
- (182) Mayer, A.; Scheglmann, D.; Dove, S.; Glatz, A.; Wickner, W.; Haas, A. *Mol. Biol. Cell* **2000**, *11*, 807–817.
- (183) Boeddinghaus, C.; Merz, A. J.; Laage, R.; Ungermann, C. *J. Cell Biol.* **2002**, *157*, 79–89.
- (184) Cheever, M. L.; Sato, T. K.; de Beer, T.; Kutateladze, T. G.; Emr, S. D.; Overduin, M. *Nat. Cell Biol.* **2001**, *3*, 613–618.
- (185) Wassarman, P. M. *Cell* **1999**, *96*, 175–183.
- (186) Blobel, C. P.; Wolfsberg, T. G.; Turck, C. W.; Myles, D. G.; Primakoff, P.; White, J. M. *Nature* **1992**, *356*, 248–252.
- (187) Wolfsberg, T. G.; White, J. M. *Dev. Biol.* **1996**, *180*, 389–401.
- (188) Cho, C.; Bunch, D. O.; Faure, J. E.; Goulding, E. H.; Eddy, E. M.; Primakoff, P.; Myles, D. G. *Science* **1998**, *281*, 1857–1859.
- (189) Chen, M. S.; Tung, K. S.; Conrod, S. A.; Takahashi, Y.; Bigler, D.; Chang, A.; Yamashita, Y.; Kincaid, P. W.; Herr, J. C.; White, J. M. *Proc. Natl. Acad. Sci. U.S.A.* **1999**, *96*, 11830–11835.
- (190) Miyado, K.; Yamada, G.; Yamada, S.; Hasuwa, H.; Nakamura, Y.; Ryu, F.; Suzuki, K.; Kosai, K.; Inoue, K.; Ogura, A.; Okabe, M.; Mekada, E. *Science* **2000**, *287*, 321–324.
- (191) Le Naour, F.; Rubinstein, E.; Jasmin, C.; Prenant, M.; Boucheix, C. *Science* **2000**, *287*, 319–321.
- (192) Miller, B. J.; Georges-Labouesse, E.; Primakoff, P.; Myles, D. G. *J. Cell Biol.* **2000**, *149*, 1289–1296.
- (193) Kaji, K.; Oda, S.; Shikano, T.; Ohnuki, T.; Uematsu, Y.; Sakagami, J.; Tada, N.; Miyazaki, S.; Kudo, A. *Nat. Genet.* **2000**, *24*, 279–282.
- (194) Löffler, S.; Lottspeich, F.; Lanza, F.; Azorsa, D. O.; ter Meulen, V.; Schneider-Schaulies, J. *J. Virol.* **1997**, *71*, 42–49.
- (195) Willett, B. J.; Hosie, M. J.; Jarrett, O.; Neil, J. C. *Immunology* **1994**, *81*, 228–233.



- (196) Taylor, M. V. *Curr. Biol.* **2000**, *10*, R646–R648.
- (197) Ruiz-Gomez, M.; Coutts, N.; Price, A.; Taylor, M. V.; Bate, M. *Cell* **2000**, *102*, 189–198.
- (198) Bour, B. A.; Chakravarti, M.; West, J. M.; Abmayr, S. M. *Genes Dev.* **2000**, *14*, 1498–1511. (a) Mohler, W. A.; Shemer, G.; del Campo, J. J.; Valansi, C.; Opoku-Serebuoh, E.; Scranton, V.; Assaf, N.; White, J. G.; Podbilewicz, B. *Dev. Cell* **2002**, *2*, 355–362.
- (199) Yagami-Hiromasa, T.; Sato, T.; Kurisaki, T.; Kamijo, K.; Nabeshima, Y.; Fujisawa-Sehara, A. *Nature* **1995**, *377*, 652–656.
- (200) Tachibana, I.; Hemler, M. E. *J Cell Biol.* **1999**, *146*, 893–904.
- (201) Berman, H. M.; Westbrook, J.; Feng, Z.; Gilliland, G.; Bhat, T. N.; Weissig, H.; Shindyalov, I. N.; Bourne, P. E. *Nucleic Acids Res.* **2000**, *28*, 235–242.

CR000036+

